Laboratory tests in borehole KFM01D, KFM08C and KFM09B

Fracture toughness using the pseudocompact tension (*p*CT) method and ultrasonic wave velocity measurements in intact rock

Jordi Delgado-Martín, Miguel Herbón-Penabad, María del Carmen García-García
Civil Engineering School, University of A Coruña

This report concerns a study which was conducted for Svensk Kärnbränslehantering AB (SKB). The conclusions and viewpoints presented in the report are those of the author. SKB may draw modified conclusions, based on additional literature sources and/or expert opinions.

Data in SKB's database can be changed for different reasons. Minor changes in SKB's database will not necessarily result in a revised report. Data revisions may also be presented as supplements, available at www.skb.se.

This report is published on www.skb.se

SVENSK KÄRNBRÄNSLEHANTERING

Abstract

This report presents the results of sixteen mode I fracture toughness tests, ultrasonic wave velocities and derived dynamic moduli performed on selected 50 mm-diameter rock specimens from the future Forsmark high-level radioactive waste repository site. The specimens were sampled from core sections obtained from three boreholes: KFM01D (sampled at a borehole length of ~397 m); KFM08C (which was sampled at two different borehole lengths: ~358 and ~550 m); and KFM09B (sampled at a borehole length of ~604 m). The tested specimens were kept submersed in tap water for one week in order to reproduce the in situ saturation conditions. Fracture toughness was determined according with the pseudo-compact tension (pCT) testing methodology. The results obtained show that, among the tested rocks, the highest value corresponds to the amphibolite of borehole KFM01D (1.93 ± 0.14 MPa m$^{1/2}$) while the lowest one is that corresponding to the albitized granodiorite of borehole KFM09B. The samples of the two different depths of borehole KFM08C display intermediate values, with the maximum value in this case corresponding to the albitized granodiorite (1.17 ± 0.08 MPa m$^{1/2}$) and the minimum to the amphibolite (1.00 ± 0.10 MPa m$^{1/2}$). With respect wave velocities, the V_P for all the samples is within 5.12 and 6.06 km/s, while the V_S ranges from 2.62 to 3.39 km/s. In both cases, the fastest propagation values correspond to the KFM01D amphibolite specimens, whose densities are also greater.

Sammanfattning

Denna rapport presenterar resultaten av sexton mod I-sprickseghetstester, ultraljudsvåghastigheter och härledda dynamiska moduler utförda på utvalda 50 mm-diameter bergexemplar från det framtida förvaret för högaktivt radioaktivt avfall i Forsmark. Proverna togs från kärnsektioner erhållna från tre borrhål: KFM01D (provtagning vid en borrhålslängd av ~397 m); KFM08C (som togs vid två olika borrhålslängder: ~358 och ~550 m); och KFM09B (provtagen vid en borrhålslängd av ~604 m). De testade proverna hölls nedsänkta i kranvatten i en vecka för att reproducera mättnadsförhållandena in situ. Frakturseghet bestämdes enligt pseudo-kompakt spänning (pCT) testmetod. De erhållna resultaten visar att bland de testade bergarterna motsvarar det högsta värdet amfiboliten i borrhålet KFM01D ($1,93 \pm 0,14$ MPa m1/2) medan det lägsta är det som motsvarar den albitiserade granodioriten i borrhålet KFM09B. Proverna av de två olika borrhålsdjupen KFM08C visar mellanvärden, där maxvärdet i detta fall motsvarar den metasomatiska granodioriten ($1,17 \pm 0,08$ MPa m1/2) och minimum till amfiboliten ($1,00 \pm 0,10$ MPa m1/2). Med avseende på våghastigheter ligger V_P för alla prover inom 5,12 och 6,06 km/s, medan V_S sträcker sig från 2,62 till 3,39 km/s. I båda fallen motsvarar de snabbaste utbredningsvärdena KFM01D amfibolitprover, vars densiteter också är större.

Contents

1   Introduction

This document reports the experimental results of mode-*I* fracture toughness (K_{IC}) tests performed with water-saturated specimens obtained from four drill core sections within the Forsmark site, corresponding to boreholes KFM01D, KFM09B, and KFM08C (Stephens et al. 2007; Waber and Smellie, 2007):

- Borehole KFM01D was drilled in the W-part of the investigation area from November 22nd, 2005, to February 18th, 2006. The borehole was intended to deliver hydrogeological and hydrochemical information about the rock volume of the central part of a potential repository area and to confirm or otherwise the existence of gently-dipping brittle zones. It was drilled at an inclination of 55° towards the NE to a total length of 800.24 meters. The drill core sample available for testing (between borehole length 397.33 to 397.60 m) is an amphibolite (rock type 102017).

- Borehole KFM08C was drilled in the northern part of the Forsmark site, at the W shore of Asphällsfjärden from April 14th, 2005 to May 9th, 2006. The borehole was intended to provide hydrogeological information from expected repository depths close to the boundary of the site investigation area. It was drilled at an inclination of 60° towards the NE, under the Baltic Sea, and to a total length of 951.1 meters. For this borehole, two drill core samples were available for testing: One corresponding to lengths going from 358.00 to 358.22 m and a second one from lengths 549.65 to 549.90 m. The shallowest section corresponds with an albitized granodiorite (rock type 101057_104) while the deepest one is an amphibolite (rock type 102017).

- Borehole KFM09B was drilled at the NW boundary of the investigation area, south of the Forsmark nuclear power plant from October 27th to December 21st, 2005. The borehole was intended to provide geological and hydrogeological information about the rock mass in a potential access tunnel area and in the central part of a potential repository. It was drilled at an inclination of 55° towards SE to a total length of 616.45 meters. The drill core sample available for testing corresponds to the length comprised between 604.00 to 604.22 m), where a fine-grained, albitized granodiorite (rock type 101057_104) occurs.

The drill core samples were sent to the Rock Mechanics Laboratory in A Coruña (Spain), where they were received on September 26th, 2024. The slicing of the cores and specimen grinding took place on October 4th. Following geometric measurements (thickness and diameter), the 16 test specimens obtained were immersed in a reservoir filled with tap water and kept at room temperature (~22 ºC) for a period of time of seven days before their testing. A final preparation stage for each sample consisted in the cut of a groove and the starter notch required to conduct the corresponding fracture toughness tests, which is the objective of this report. In addition, ultrasonic velocity measurements (V_P and V_S) were also performed with the saturated specimens prior to fracture toughness testing. The information obtained provides with site-specific data useful to elaborate more accurate geomechanical models and predictions. Both aspects contribute to a better characterization and understanding of the behaviour of granitic rocks in Forsmark within the context of the ongoing engineering and safety studies for the disposal of spent nuclear fuel conducted by SKB.

2 Materials and Methods

2.1 Drill Cores and Specimens Preparation

Four 50 mm-diameter drill cores were transferred from the Forsmark site to the *Rock Mechanics Laboratory, LaMeRoc*. Figure 2-1 presents some images of the cores received before cutting and trimming. In order to make possible the correct top/bottom orientation of the sliced samples, two parallel (blue and red) lines were marked following their axis.

Specimens were pre-cut from the drill cores using a 350 mm-diameter diamond saw disk (*Carat* mod. P-3500) and then trimmed with a manual drill (*Optimum BF-16V*) equipped with a lapping diamond disk to ensure flatness and parallelism between opposed faces. Tap water was used in all the preparation procedures. Figure 2-2 shows a photographic sequence of the slicing of the cores.
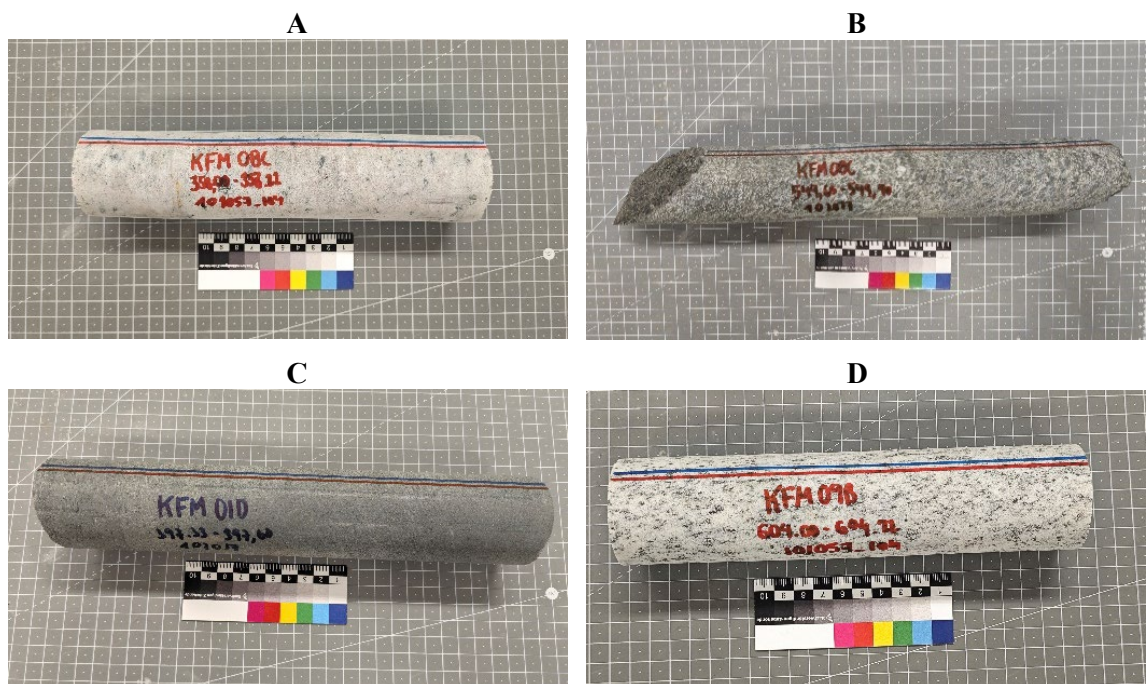

Figure 2-1 Drill cores received by LaMeRoc on September 26th, 2024. A: KFM08C (borehole length 358.00 to 358.22 m; rock type 101057_104). B: KFM08C (borehole length 549.65 to 549.90 m, rock type 102017). C: KFM01D (borehole length 397.33 to 397.60 m; rock type 102017). D: KFM09B (borehole length 604.00 to 604.22 m, rock type 101057_104). Cores are oriented with their left side pointing towards the shallowest depth (Adj Secup)

The dimensions of the trimmed specimens were determined with the aid of a Vernier calliper (*Mitutoyo mod. 500-197-20*; resolution = 0.01 mm). Before the determinations, the calliper was checked using a reference length standard of 25.4 mm length and 12.7 mm diameter.

In compliance with the Method Description for determining density and porosity of intact rock, SKB MD 160.002e (internal SKB document), all the specimens were immersed during 7 days in a covered reservoir filled with tap water kept at room temperature (~22 ºC) and ambient pressure (Figure 2-3). Then, the weight of the specimens was determined with the aid of an internally calibrated digital scale (*Sartorius Entris 4502*; precision = 0.01g) which was further verified with a reference standard weight.

No information was available about the moisture condition of the received drill cores and they were not oven-dried. Therefore, the data reported in this document related with the mass and density correspond to that of the samples in their wet/saturated condition (Figure 2-3).

Table 2-1 summarizes some relevant information related with the samples, including their location within the corresponding drill cores, average thickness and diameter or the apparent (moist) density.
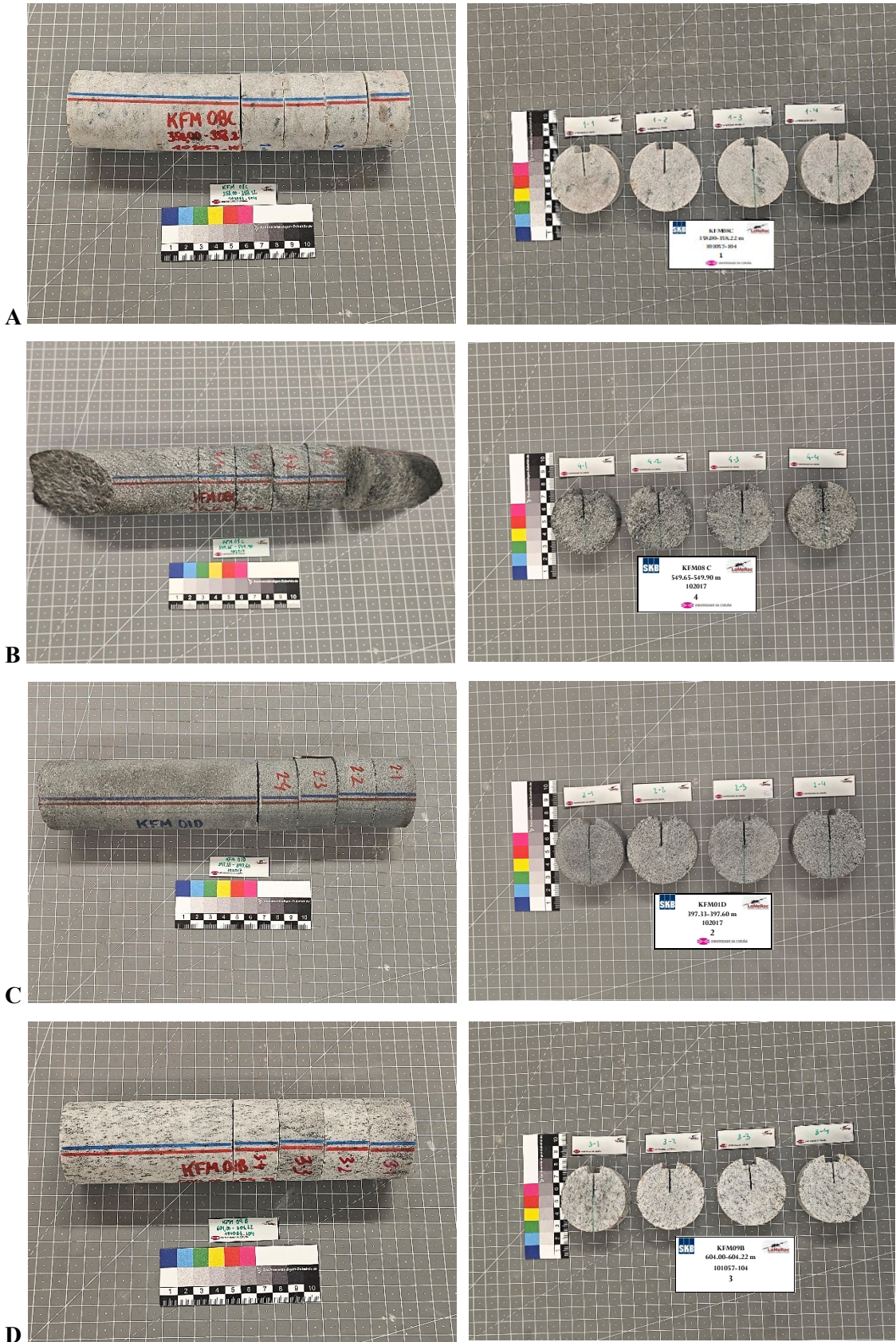
Figure 2-2 *Sliced drill cores (left) and the corresponding specimens obtained for testing (right).* **A:** KFM08C. **B:** KFM08C. **C:** KFM01D. **D:** KFM09B. *Cores are oriented in with their left side pointing towards the shallowest depth (Adj Secup)*

Figure 2-3 *Sliced specimens while immersed in tap water (left) and measurement of their corresponding geometric dimensions and weight (right)*

Table 2-1. Approximate location of the specimens within the boreholes KFM08C, KFM01D and KFM09B and some of their representative properties.

Borehole	Specimen	Adj Secup (m)	Adj Seclow (m)	L_{mean} (mm)	D_{mean} (mm)	L/D (–)	M (g)	ρ (kg/m^3)	ρ_{mean} (kg/m^3)
KFM08C	1-1	358.00	358.03	25.87	50.94	0.51	137.98	2617	2605 ± 6
	1-2	358.03	358.06	27.05	50.88	0.53	142.47	2590	
	1-3	358.06	358.08	25.62	50.98	0.50	135.95	2599	
	1-4	358.09	358.11	26.20	50.99	0.51	139.81	2613	
KFM08C	4-1	549.70	549.73	27.13	50.78	0.53	160.52	2921	2954 ± 14
	4-2	549.73	549.76	27.05	50.79	0.53	161.33	2944	
	4-3	549.76	549.79	26.90	50.77	0.53	162.36	2982	
	4-4	549.79	549.82	26.69	50.92	0.52	161.39	2970	
KFM01D	2-1	397.33	397.36	27.30	50.39	0.54	158.58	2912	2928 ± 6
	2-2	397.36	397.39	26.19	50.41	0.52	153.02	2927	
	2-3	397.39	397.42	26.45	50.51	0.52	155.60	2935	
	2-4	397.42	397.45	26.59	50.44	0.53	156.00	2936	
KFM09B	3-1	604.00	604.03	27.01	50.91	0.53	143.39	2608	2618 ± 4
	3-2	604.03	604.06	26.36	50.91	0.52	140.75	2624	
	3-3	604.06	604.09	26.45	50.94	0.52	141.30	2621	
	3-4	604.09	604.12	26.45	50.94	0.52	141.28	2621	

Notes: **Adj Secup** = top level of the specimen referred to borehole length; **Adj Seclow** = bottom level of the specimen referred to borehole length; **L_{mean}** = mean thickness; **D_{mean}** = mean diameter; **L/D** = slenderness ratio; **M** = wet mass; **ρ** = bulk density; **ρ_{mean}** = bulk mean density ± standard error of the mean

2.2 Mode I Fracture Toughness Testing with the *p*CT Method

SKB has not defined a specific protocol for fracture toughness testing. To conduct the experimental work, we have followed general recommendations outlined by the ISRM (ISRM, 1988) as well as internal laboratory procedures elaborated at the time of development of the *p*CT method (Muñoz-Ibáñez et al., 2020). This method has been previously compared with the ISRM-suggested semi-cylinder bending (SCB) method (Kuruppu et al. 2014) in the SKB report P-21-02 (Delgado et al., 2021). Guidelines for data reporting were kept consistent with those described by SKB for other testing methods, e.g. SKB MD 190.001e and SKB 190.004e, for uniaxial compressive strength (UCS) and indirect tensile strength (ITS) testing, respectively.

As it was described in the previous sections, the samples selected for testing were submersed during 7 days in tap water and then extracted (one by one) to cut a U-shaped groove (along the cylindrical surface of the sample; 10 mm-width and 5 mm-depth) and a centered starter notch (1 mm-width and ~17 mm-depth). The cuts, which were made just before each test, were performed with a modified tile saw equipped with a diamond disk.

In previous tests, the length of the starter notch was shorter (11 mm) than that used in the present survey (17 mm). The reason for that was to ensure a better control in the direction of propagation of the crack, what allows for a more precise assessment of crack energy distribution in the case that this were necessary. In any case, the extended starter notch length is within the recommended size bounds given by Muñoz-Ibáñez *et al.* (2020). Starter notch length effects have been investigated by Muñoz-Ibáñez et al. (2021) and, for the limited range of change considered, they are not expected to affect the results and/or the comparability with those obtained in previous surveys.

2.2.1 Fracture Toughness Test Equipment and Procedures

According to ISRM (1988), fracture toughness investigations in rocks can be conducted with the suggested methods according to two testing levels:

- Level I (or screening level) provide fast and relatively simple access to material properties. In this level, only the maximum load (P_{max}) needs to be measured.
- Level II (or advanced level) takes into account the non-linear behavior that many rocks present. That level allows for a more detailed insight about the mechanics of the fracturing processes by continuously monitoring both the load and displacement beyond P_{max}.

Although the equipment described next can perform both levels of testing, for the present survey we only report results based on Level I testing. Reasons for that are described in following paragraphs.

The pseudo-compact tension (*p*CT) test (Muñoz-Ibáñez et al., 2020; Delgado et al., 2021) is based on an adaptation of the compact tension (CT) specimen described in the E399-12 ASTM standard method (ASTM, 2012) for testing metallic materials and its testing principle is outlined in Figure 2-4 and Figure 2-5 in the *p*CT configuration, the two loading holes of the CT specimen are replaced by a U-shaped groove. In addition, a thin radial notch is cut to act as stress concentrator and to provide the location for crack initiation.

Once the specimen is ready for testing, carrying out the test follows a simple and straightforward procedure. The specimen is mounted on a centering cradle and put in contact with a pair of high-strength, high-stiffness steel jaws that fit into the U-shaped groove and transmit the tensile load to the sample. While one of the jaws remains in a static position, the other one is pulled apart at a constant displacement rate. The tensile load within the thin notch tends to split the specimen into two symmetrical halves. The crack initiates at the notch tip and propagates along the vertical diameter of the specimen (i.e. the ligament plane). With this basic configuration, the bottom of the sample is not affected by other loads that its own self-weight.
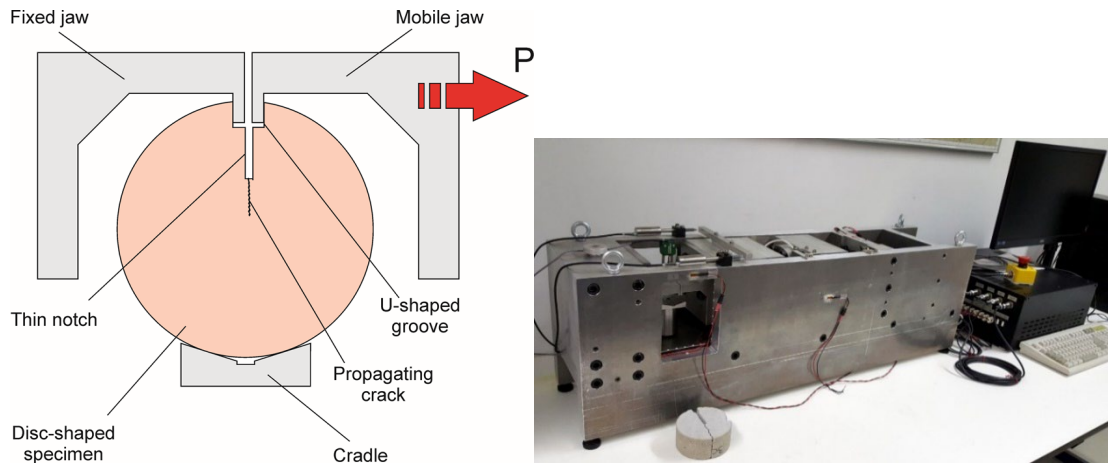
Figure 2-4 *Conceptual scheme of the pCT test (left) and frame used to conduct the experiments.*

The testing device consists of a high-stiffness frame (alloy AA7075-T6; E = 71.7 GPa, ν = 0.33, σ_{yield} = 503 MPa) equipped with a 50 kN push/pull load cell (*AEP Transducers mod. CTC412750KNI15*), two linear variable differential transducers (*Solartron LVDT G-series AX/5/S*), and two clip-on (COD) gages (*Epsilon Technology Co.* mod. 3541 and *MTS Co.* mod. 632.02).

Electric signals from all the measurement devices are integrated into a dedicated data acquisition system (*GW Instruments Inc.* instruNet 3.6). The two LVDTs, placed symmetrically on both sides on the specimen, measure the load point displacement (LPD). Simultaneously, a clip-on gage mounted on a pair of bolt-on knife edges attached to the steel jaws measures the same magnitude for redundancy. An additional COD gage can be mounted directly on the surface of the specimen to measure the crack mouth opening displacement (CMOD) although in the *p*CT configuration CMOD can be readily compared with LPD.

The movement of the steel jaw is accomplished by means of a 5-mm lead spindle (NBS mod. VFU 40005 DIN 69051 Form B), which converts the rotary motion of an electric stepper motor (*Teco Electro Devices Co.* mod. DST56EL61A) with a step-angle of 1.8° (i.e., 200 steps per revolution) into linear displacement. To improve its performance, the motor is connected to a planetary gearhead (*McLennan Servo Supp.* mod. IP-57-M2-100) with a reduction ratio of 1:100. This configuration provides a high degree of accuracy in positioning (0.018°/step), equivalent to 0.25 μm/step in terms of linear movement of the shaft, which can be maintained from 0 to 50 kN.

The control system consists of: (i) an Arduino-based microcontroller (which commands the motor with a specific program, and keeps track of the displacements and safety signals delivered by the end-stops) and (ii) dedicated software (that makes it possible to set up a testing path). Control commands are transmitted in real time to the microcontroller, which executes them and returns state and displacement data.

A stainless-steel bellow coupling with a clamping hub (*StS Couplings* mod. WK4/60-89-SX 49/15,) connects the motor and the spindle. A fixed-side round-type support bearing (*Hiwin* FK30-C5) provides both axial and rotational support for the spindle.

The data files obtained after each test were later filtered and post-processed in order to obtain the required properties. Post processing was performed with the aid of different *Microsoft*[TM] *Excel*[®] worksheets and plotting with the software *Grapher*[®] 12.7 by *Golden Software Inc*.

Characteristics of the Specimens

The *p*CT specimen is a cylindrical, disc-shaped sample that can be cut from rock cores. Its geometrical properties are summarized in Figure 2-6. This is based on the work of Muñoz-Ibáñez et al. (2020). According with the prescriptions outlined there, the *p*CT samples should have a recommended diameter of 50 mm and a thickness to diameter (L/D) ratio of 0.5. Table 2-2 summarizes the geometric properties of the tested samples.

Testing Procedures

*p*CT tests were executed according to the guidelines indicated by Muñoz-Ibáñez et al. (2020) and these are summarized in Table 2-3. For fracture toughness investigations in rocks, the two aforementioned testing levels, Level I (or screening level) and Level II (or advanced level), are commonly reported in the literature (ISRM, 1988). Although the features and characteristics of the testing equipment are compatible with Level II, according with the considerations presented in section 2.4, the interpretation of tests will be made based on Level I.

Table 2-2. Properties of the specimens used for *p*CT fracture toughness testing.

Group	Specimen	D_{mean} (mm)	a (mm)	G_d (mm)	b (mm)	B (mm)	a/b (–)
KFM08C	1-1	50.94	17.01	6.14	44.80	25.87	0.38
	1-2	50.88	17.16	5.73	45.15	27.05	0.38
	1-3	50.98	17.85	5.79	45.19	25.62	0.39
	1-4	50.99	17.57	5.47	45.52	26.20	0.39
KFM08C	4-1	50.78	17.84	5.53	45.25	27.13	0.39
	4-2	50.79	17.01	5.79	45.00	27.05	0.38
	4-3	50.77	17.21	5.41	45.36	26.90	0.38
	4-4	50.92	17.71	5.89	45.03	26.69	0.39
KFM01D	2-1	50.39	17.11	5.76	44.63	27.30	0.38
	2-2	50.41	17.81	5.04	45.37	26.19	0.39
	2-3	50.51	17.92	4.90	45.61	26.45	0.39
	2-4	50.44	17.65	5.19	45.25	26.59	0.39
KFM09B	3-1	50.91	17.85	6.01	44.90	27.01	0.40
	3-2	50.91	17.69	5.16	45.75	26.36	0.39
	3-3	50.94	17.19	5.88	45.06	26.45	0.38
	3-4	50.94	17.09	5.78	45.16	26.45	0.38

Notes: D_{mean} = mean diameter; **a** = starter notch length; G_d = groove depth; **b** = notch length ratio; **B** = specimen thickness.
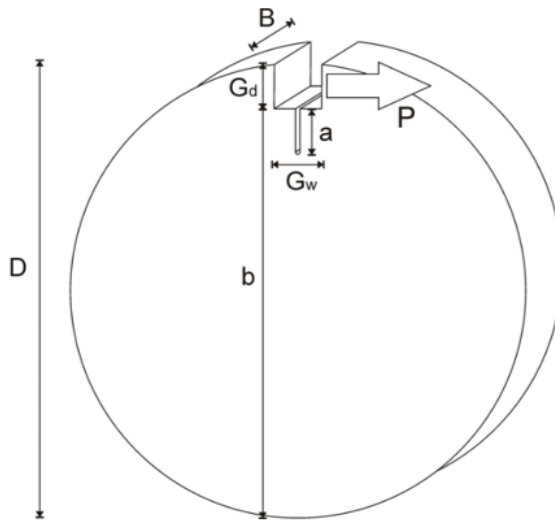

Figure 2-5 *Schematic illustration of the geometry of the pCT specimen. Notes: P = applied horizontal load; D = specimen diameter; B = specimen thickness; a = starter notch length; G_d = groove depth; G_w = groove width; b = distance from the base of the groove to the bottom of the specimen.*

Table 2-3. *p*CT testing procedure.

Step	Description
1	Digital photographs of the specimen are taken before test execution.
2	The specimen is placed on the positioning cradle and then lifted until the steel jaws fit into the groove. The height of the cradle is manually controlled using a positioning spindle.
3	The verticality of the specimen is checked using a self-levelling cross-line laser.
4	The stress (load) and LPD (linear displacement sensor) measurement channels are zeroed in the data acquisition software.
5	The beginning of the test is concurrent to recording. Recorded data includes load and load point displacement (LPD). When the loading force starts to rise the support cradle is lowered to ensure an unconstrained behavior in the specimen. The test is executed in displacement-control mode at a constant rate of 0.1 mm/min (0.0017 mm/s).
6	The test is stopped manually (switch off) after peak load has been observed and the applied force has drop to a level close to the starting one.
7	Digital photos are taken of the specimen upon completion of each test.
8	The testing device is disassembled and carefully cleaned for the next test.

Data Processing

Following Muñoz-Ibáñez at al. (2020), the computation of K_{IC} (in MPa m1/2) for the *p*CT testing method can be performed according to the following equation:

$$K_{IC}^{pCT} = Y'_{pCT} \sigma_{max} \sqrt{\pi a}$$

where σ_{max} is the applied stress at the critical load ($\sigma_{max} = P_{max}/(bB)$; in MPa) and B the thickness of the specimen (in m). In order to compute the specific non-dimensional stress intensity factor Y'_{pCT}, these authors provide the following equation:

$$Y'_{pCT} = C_0 + C_1 \left(\frac{a}{b}\right) + C_2 \left(\frac{a}{b}\right)^2 + C_3 \left(\frac{a}{b}\right)^3 + C_4 \left(\frac{a}{b}\right)^4$$

The coefficients C_i ($i = 0$ to 4) to compute the stress intensity factor are given in Table 2-4.

Table 2-4. Coefficients for the computation of the specific non-dimensional stress intensity factor Y'_{pCT} of the pCT fracture toughness testing method.

D (mm)	C_0	C_1	C_2	C_3	C_4
38	10.278	-24.069	82.329	-136.670	127.890
50	12.651	-47.054	158.720	-247.170	185.220
100	15.341	-74.551	260.030	-404.520	273.190

2.2.2 Assessment of the validity of fracture toughness test results

The assessment of the validity of fracture toughness results based on Level I testing requires the fulfilment of some acceptability criteria whose application have not been yet sufficiently discussed in rocks. In order to establish the minimum criteria for the acceptability of the test results, we have considered two complementary approaches: the application of the *compliance (or 5% secant)* method (which is covered, among others, by the standard ASTM E399-12; ASTM, 2012) and the plane-strain criterion check.

The secant compliance method seeks to verify the applicability of the linear elastic fracture mechanics (or LEFM) postulates. A 5% secant line with a slope equal to 95% of the initial elastic loading slope is normally used to determine P_5 or P_Q.

This slope would correspond approximately with the load required to generate a ~2% (or less) apparent crack extension in the type of materials covered by the reference standards.

Compliance method criterion

Figure 2-6 illustrates the application of the compliance method to check the applicability of the linearity condition supporting the computation of K_{JC} based on Level I fracture toughness testing. The plot corresponds to sample 1-3 of drill core KFM06A-1. The procedure for its application is as follows:

- A linear best fit line is computed to the linear loading segment of the experimental P-CMOD curve to determine the initial compliance (Θ). This is given by the reciprocal of the slope of line AB.
- A second line, AB', is draw with a compliance 5% greater than that of line AB.

The experimental data provides with a P_{max} value (maximum load that the specimen was able to sustain during the test) and the intersection of line AB' with the experimental curve identify the so-called conditional load or P_Q. Based on these references it is possible to compute a P_{max}/P_Q ratio that, if smaller than 1.10, supports the applicability of the LEFM hypotheses. In the case that it was larger, then an elastoplastic approach (Level II) would be required to characterize K_{JC} as a material property. In the case of the example illustrated the P_{max}/P_Q ratio is 1.01 what makes possible the computation of K_{JC} associated with Level I fracture toughness testing.
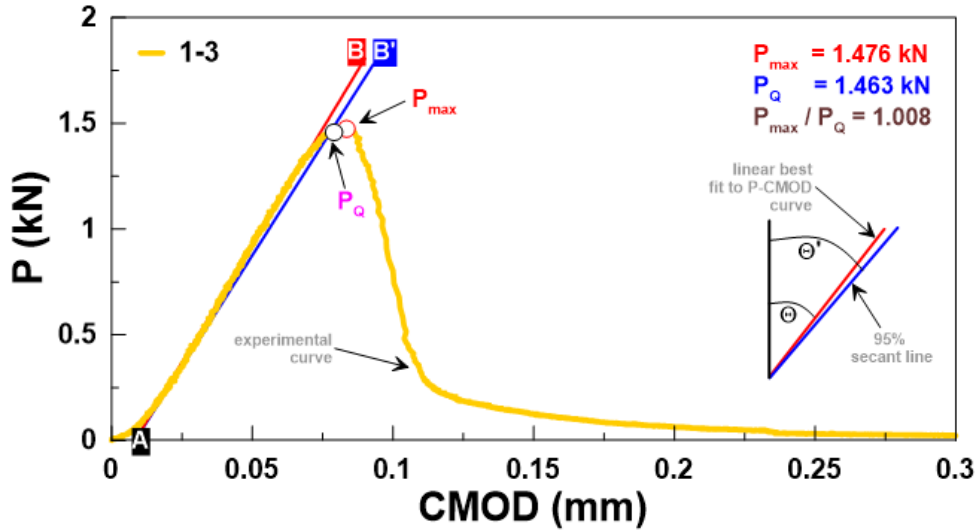
Figure 2-6 *Experimental results corresponding a pCT test used to verify the linearity criterion of the compliance method. See text for explanation. Notes: P = applied horizontal load; P_{max} = maximum load; P_Q = conditional load; CMOD = crack mouth opening displacement ($\equiv$ load point displacement in the pCT test); Θ = compliance angle; Θ' = compliance angle of the 95% P-CMOD slope.*

The ASTM E399 standard also identifies situations in which P_{max} is located between the curves AB and AB' curves and when it lays ahead of the AB' line. In the first case, the computation of K_{IC} can be directly performed based on the P_{max} value while in the second, the prescribed value to use is P_Q. Based on that, what we obtain in each case is a conditional value K_Q (that is derived from P_Q) or the true mode-I fracture toughness K_{IC} (when using P_{max}).

Plane-strain criterion

The ASTM E399 standard pays also attention to the fulfilment of plane-strain conditions to determine a K_{IC} value amenable of consideration of a true material property. To this respect, sample thickness is a key property as it affects how the plastic domain around the crack tip (or fracture process zone, FPZ) is fully developed within the body of the specimen (i.e. its outer boundaries are not strained) or if it interacts with them. As a rule of thumb the minimum diameter (D) of the tested sample should keep in line with the following relationship:

$$D \geq 2(K_{IC}/T)^2$$

where T represents tensile strength. This expression is derived from theoretical considerations on the size of the fracture process zone (L_{FPZ}), which is considered to be proportional to the square ratio of K_{IC} and T:

$$L_{FPZ} \propto (K_{IC}/T)^2$$

The application of the plane strain criterion is not straightforward because, although we may have an estimation of T, the computation of K_{IC} requires the testing of specific specimens. However, due to the impracticability of conducting a specific survey addressing the thickness-dependence of K_{IC} in the particular rock tested, we have considered an indirect approach based on the assessment of the L_{FPZ}. This involves the geometrical properties of the samples, the K_{IC} values computed after their testing and the estimated value of T, which in this study is assumed to correspond to that of rocks type 102017 and 101057_104. Thus, the size of the computed L_{FPZ} can be compared with the thickness of the sample and the ligament length (distance b-a in Figure 2-5); this way, if the L_{FPZ} results to be larger than these two properties, then the plane strain condition is challenged and the K_{IC} value would be inaccurate.

Different researchers have considered diverse approaches to compute L_{FPZ} (e.g. Dutler et al. 2018 and references therein). Worth mentioning among them are the basic model of Irwin ($L_{FPZ,I}$), the strip-yield uniform traction model ($L_{FPZ,SU}$) and the strip-yield linear traction model ($L_{FPZ,ST}$). The corresponding expressions are given as follows:

$$L_{FPZ,I} = \frac{1}{\pi}\left(\frac{K_{IC}}{T}\right)^2 \qquad L_{FPZ,SU} = \frac{\pi}{8}\left(\frac{K_{IC}}{T}\right)^2 \qquad L_{FPZ,ST} = \frac{9\pi}{32}\left(\frac{K_{IC}}{T}\right)^2$$

2.3   Ultrasonic Wave Velocity Determinations (V_P and V_S)

Ultrasonic pulse velocities (V_P and V_S) were determined by capturing waveforms with the aid of two *ErgoTech Ltd.* 1.5" (38.1 mm) Ti-faced compression platens (Figure 2-7). This system is equipped with acoustic ultrasonic emitter/receivers whose central frequency is 1.3 MHz. The PZT5a piezoelectric stack of the emitter is excited with a high-voltage source located in a quadratic pulse generator also manufactured by *ErgoTech Ltd*. The receiver unit is identical to the emitter so their role can be exchanged. The transducers make possible the observation of the travel time of compressional (P) and two orthogonally-polarized shear waves (S_1, S_2). For each sample and wave-type (either P, S_1 or S_2) a total of 32 waveforms were recorded, digitized, stacked (to reduce noise) and processed with the aid of a *Pico Technology 5252B*, 200 MHz bandwidth digital oscilloscope and the *PicoScope*® software (ver. 6.14.5.4585).

Figure 2-7 *Platens and load frame used to perform the ultrasonic pulse velocity determinations of the Forsmark site borehole specimens.*

To conduct the measurements, the specimens were installed between the transducer platens which, in turn, are mounted in a dedicated load frame equipped with a manual hydraulic actuator (*Enerpac RC106*) and a 100 kN load cell (*AEP Transducers mod. CCBS8210T5*). The general procedure for ultrasonic velocity measurements requires to test the samples at room temperature using a coupling media while applying a certain load (~1 kN) to ensure a good contact between the transducers and the plug being tested.

In order to improve contact and detection of travel times of the seismic waves, all the samples were loaded to a corresponding stress of 1 MPa (i.e. correcting the load according to the surface of the specimen). Furthermore, to enhance the physical contact, a thin layer of *Olympus SWC-2* shear wave couplant was used to improve shear wave detection. The experimental method makes possible the determination of the time-of-flight (TOF) of an ultrasonic pulse traveling through the tested rock.

There is no SKB recommended single procedure to evaluate both ultrasonic velocities, V_P and V_S, in core plugs. However, there are two main standard procedures applicable to measurements in rocks: ASTM D2845-05 (ASTM, 2005) and the Suggested Method of the *International Society for Rock Mechanics and Rock Engineering*, ISRM (Aydin et al., 2014). While the D2845-05 standard provides with technical guidelines, it does not include any provision for checking the performance of the transducer elements.

The ISRM suggested method emphasizes the importance of TOF correction due to the delay imposed by the presence of face platens and provides with several ways to account for it. None of them make any consideration with respect the methodology for the picking of the first arrival of P and S waves which is, in fact, the most critical aspect in order to determine ultrasonic velocities. In summary: There is no strict recommendations or standard guideline for the verification of transducers and the procedures followed at *LaMeRoc* conform to best practices based on the experience. They are based on two main procedures and checks and they are aimed at ensuring the highest reliability in the obtained waveforms. They are summarized next:

2.3.1 Procedure to Check of the Good Operation of the Transducers

To check the good performance of the ultrasonic transducers, a preliminary test was performed to assess the TOF value associated to the direct contact of the platens (i.e. without the presence of any sample). The measured TOF can be compared with the data stated by the manufacturer at the time of the reception of the equipment. Although this determination should constitute an instrumental constant, the periodical check of the transducers provides information about the eventual drift associated with damage in some of the crystals of the transducer stack.

2.3.2 Verification of Ultrasonic Transducers

A series of internal verification plugs are available at *LaMeRoc*. They are made of different materials (aluminium and steel alloys, brass, PMMA) with different diameters and lengths. This verification procedure consists in the comparison of the obtained V_P & V_S values with the expected ones for the corresponding materials. In the case of the tests performed, we used a 6082-T6 (UNE L-3453) aluminium alloy plug of 38.1mm-diameter and equal length. There is no literature available about the specific wave velocity values of this particular alloy although it is well known that aluminium alloys typically have a V_P of ~6300 m/s and V_S of ~3100 m/s. A summary of the properties of this reference material is provided in Table 2-5.

2.3.3 Acquisition Conditions

The conditions for waveform acquisition consider the following settings: a) Lowpass (1 MHz) filtering; b) 4 MS/s sampling; c) 15-bit resolution; d) 10 and 20 µs/div acquisition times (for P and S waves, respectively); e) 32 averaged stacked waveforms.

Table 2-5. Selected properties of the aluminum alloy 6082-T6 (UNE L-3453) used to check the ultrasonic transducers

Chemical Composition (%)		Geometrical and mechanical properties	
Si	0.70 – 1.30	Young's modulus	69.5 MPa
Fe	0.50	Poisson's ratio	0.33
Cu	0.10	Density	2710 kg/m^3
Mn	0.40 – 1.00	Yield strength	270 MPa
Mg	0.60 – 1.20	Brinell's hardness (HBS)	94
Cr	0.25		
Zn	0.20	Diameter	38.1 mm
Others	0.10	Length	38.1 mm

2.3.4 Waveform Processing

All the waveforms were acquired and processed in the same way. Figure 2-8 presents an example corresponding to specimen 2-4 of borehole sample KFM01D. For each P, S_1 and S_2 measurement, a total of 48 waveforms are recorded. After their acquisition, the set of 48 waveforms were stacked and averaged to reduce noise. The averaged waveform was then amplitude-normalized by its mean according to the following formula:

$$x' = \frac{x - \bar{x}}{x_{max} - x_{min}}$$

In order to reduce the bias inherent to the manual picking of the TOF, we have applied a semi-automatic picking algorithm based on the Auto Regressive Akaike Information Criterion (AR-AIC). By applying the AIC method, it is assumed that the intervals before and after wave-phase arrival (either P or S) correspond to two different stationary processes separated by an onset (arrival time) where the AIC characteristic function (CF) attains a minimum value. Before computing the CF, the normalized waveform is smoothed by applying median filter the AIC-picker algorithm, a median-filter is applied to the normalized waveform. The general formulation of the AIC model is as follows:

$$AIC(k) = (k - M) \cdot log(\sigma_{1,max}^2) + (N - M - k) \cdot log(\sigma_{2,max}^2) + C_2$$

where M is the length of the auto-regressive filter, $\sigma^2{}_{1,max}$ and $\sigma^2{}_{2,max}$ are the variances of the time series in intervals $[M+1,k]$ and $[k+1,N-M]$, and C_2 is a constant.

In our case, the AIC characteristic function has been computed following the method described in Maeda (1985). This is obtained directly from the waveform without computing the coefficients M and C_2 through the following expression:

$$AIC(k) = k \cdot log\{var(x[1,k])\} + (N - k - 1) \cdot log\{var(x[k + 1, N])\}$$

where $var(x[1,k])$ is the variance of the time series $x(1)$, $x(2)$,…, $x(k)$, and $var(x[k+1,N])$ is the variance of the time series $x(k+1)$, $x(k+2)$, …, $x(N)$. The previous computations were implemented in a *Microsoft*^{TM} *Excel*® worksheet where the time window of interest (i.e. where the pulse arrival is expected to occur) is defined by the operator as an "educated guess".

Once the arrival time is known, TOF can be computed and corrected by subtracting the delay time (T_{blank}) associated to the travel of the pulse through the thickness of the transducer platens previously obtained from a face-to-face measuring test. The corresponding velocity formula is the following:

$$V = \frac{TOF - T_{blank}}{L_{mean}}$$

where V is the computed velocity (either P or S) and L_{mean} the length of the travel path.
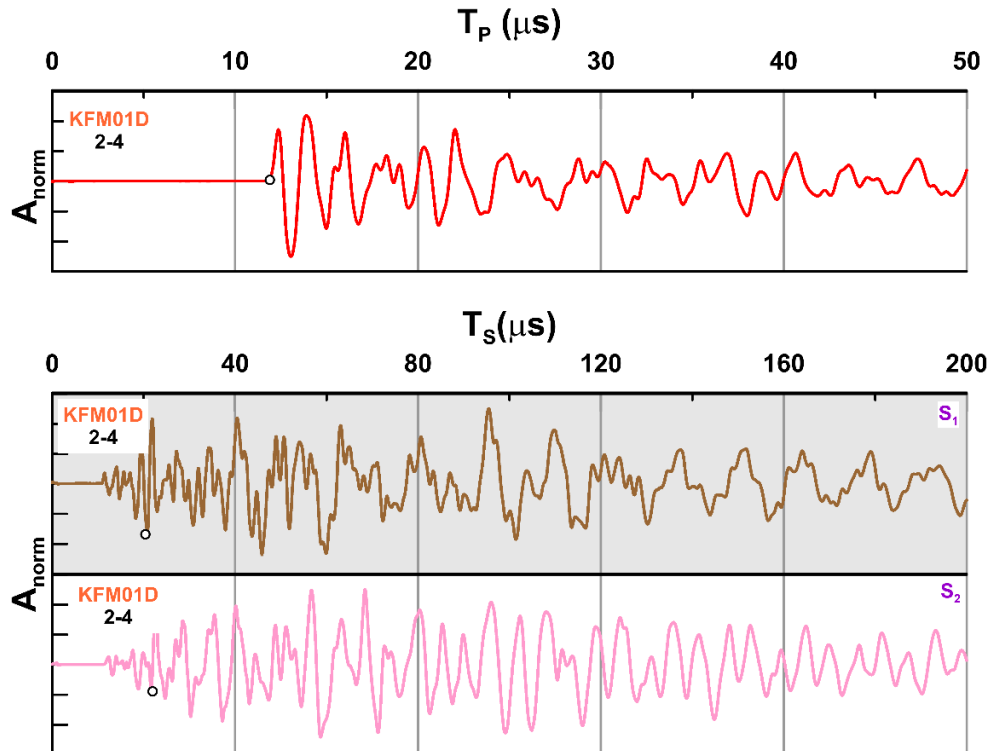
Figure 2-8 *Example application of the AIC picking methodology described in the text to P- and S-type waveforms (top and bottom, respectively). The lines correspond to the normalized waveforms and the empty dot locates the arrival time obtained with the AIC algorithm. The waveforms correspond to specimen 2-4 of borehole KFM01D.*

2.3.5   Assessment of Dynamic Moduli

The computation of dynamic moduli is based on the experimental measurements and the formulas described in the standard ASTM D2845-05. These are the followings:

- Dynamic Young's modulus:

$$E_{dyn} = 3\rho_{app}V_S^2 \frac{V_P^2 - \frac{4}{3}V_S^2}{V_P^2 - V_S^2}$$

- Dynamic Poisson's ratio:

$$\upsilon_{dyn} = \frac{1}{2}\left\{ 1 - \frac{1}{\left(\frac{V_P}{V_S}\right)^2 - 1} \right\}$$

- Dynamic Shear modulus:

$$G_{dyn} = \rho_{app}V_S^2$$

- Dynamic Bulk modulus:

$$K_{dyn} = \rho_{app}\left(V_P^2 - \frac{4}{3}V_S^2\right)$$

where ρ_{app} represents the apparent density of the rock (bulk density in our case), V_P the longitudinal (compressional) velocity and V_S the shear pulse velocity. If density units are given in kg/m^3 and velocities in m/s, the corresponding units for the Young's, shear and bulk moduli are N/m^2.

2.4   Statistic Treatment and Data Reduction

Due to the small number of tests performed (4 groups of specimens with 4 samples each), it is not possible to perform any comprehensive statistical assessment and the results are only presented in terms of their arithmetic average ($\bar{X}$) and associated standard error of the mean (SE), which are computed as follows:

$$\bar{X} = \frac{\sum_1^n x_i}{n} \qquad SE = \frac{S}{\sqrt{n}}$$

for which S represents the standard deviation and n the number of samples.

3 Results

The average bulk densities of the tested rocks after seven days of immersion in tap water are presented in Table 3-1. This value is higher in the case of the amphibolite rocks.

Table 3-1. Average density (± standard error of the mean) of the tested specimens after 7 days immersion in tap water.

Borehole	Adj Secup (m)	Adj Seclow (m)	Rock Type	Specimens	ρ_{mean} (kg/m^3)
KFM08C	358,00	358,22	101057_104	1-1, 1-2, 1-3, 1-4	2605 ± 6
KFM08C	549,65	549,90	102017	4-1, 4-2, 4-3, 4-4	2954 ± 14
KFM01D	397,33	397,60	102017	2-1, 2-2, 2-3, 2-4	2928 ± 6
KFM09B	604,00	604,22	101057_104	3-1, 3-2, 3-3, 3-4	2618 ± 4

Note: Rock types 102017 and 101057_104 are amphibolite and albitized granodiorite, respectively. ρ_{mean} = bulk mean density.

Figure 3-1 shows the experimental results obtained, while each specific experiment is documented in the Appendix 2. It was indicated previously that, in the absence of specific recommendations to assess the acceptability of fracture toughness test results in rocks, we have defined a procedure to conduct a two-step check based on the plane strain (estimated length of the fracture process zone L_{FPZ}) and the compliance (5% secant line slope method) criteria. According to them, Table 3-2 shows the assessment of the length of the fracture process zone in the tested samples according to three different models. We see that, when considering the samples, both thickness and ligament length (b-a; see Figure 2-5) are significantly larger than the computed L_{FPZ}, indicating that the samples satisfy the plane-strain constrain.

On the other hand, Table 3-3 shows the results of the assessment of the P_{max}/P_Q ratio for all the tested samples and methods (see also Appendix 2 for their graphical representation). We see that, for all the tested specimens, this ratio is below the 1.10 threshold value, what would confirm the applicability of LEFM approach to the computation of K_{IC} in Level I testing. Moreover, since P_Q lays in the experimental curves slightly before than P_{max}, the conditional load must be considered to compute the conditional fracture toughness, K_Q. In fact, the closeness of P_Q to P_{max} determines that the numerical values of K_Q (computed with P_Q) and K_{IC} (computed with P_{max}) are virtually the same, which makes possible to conclude that $K_Q \sim K_{IC}$.
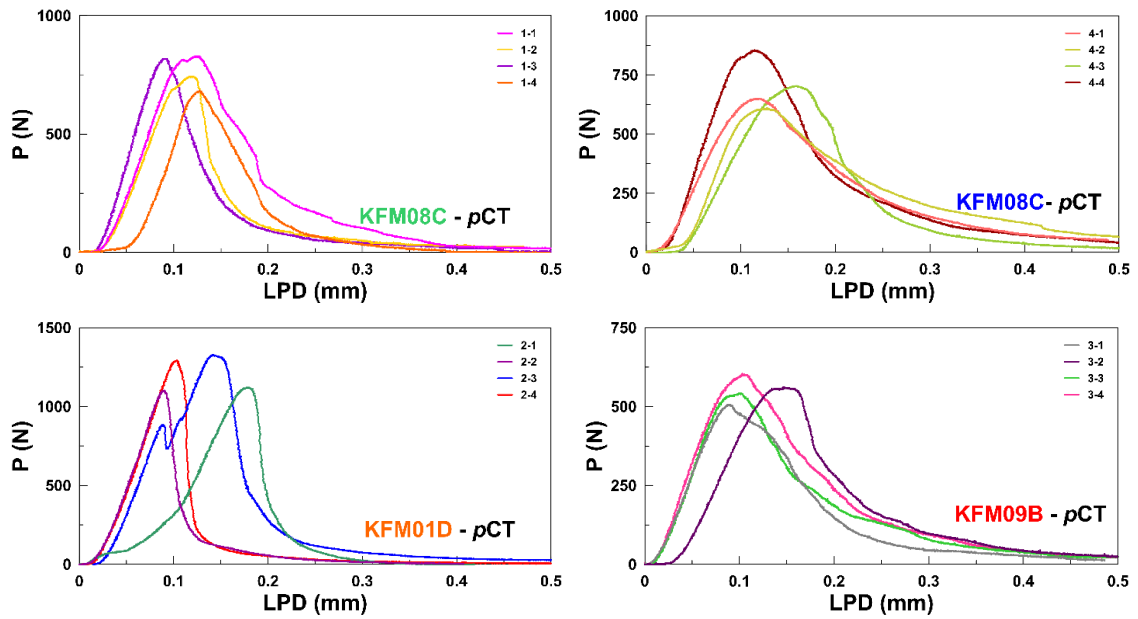
Figure 3-1 Load vs. load point displacement (LPD) curves associated with the sixteen fracture toughness tests performed with specimens of boreholes KFM08C, KFM01D and KFM09B.

Table 3-2. Assessment of the length of the fracture process zone according to the Irwin's ($L_{FPZ,I}$), strip-yield uniform traction ($L_{FPZ,SU}$) and the strip-yield linear traction ($L_{FPZ,ST}$) models.

Group	Specimen	$L_{FPZ, Irwin}$ (mm)	$L_{FPZ, SU}$ (mm)	$L_{FPZ, ST}$ (mm)
KFM08C	1-1	2.55	3.14	7.07
	1-2	1.78	2.19	4.93
	1-3	2.74	3.38	7.61
	1-4	1.82	2.25	5.06
KFM08C	4-1	1.40	1.73	3.89
	4-2	1.14	1.41	3.17
	4-3	1.54	1.90	4.28
	4-4	2.54	3.13	7.05
KFM01D	2-1	4.65	5.74	12.91
	2-2	5.06	6.24	14.03
	2-3	7.89	9.74	21.91
	2-4	6.70	8.27	18.60
KFM09B	3-1	0.99	1.22	2.74
	3-2	1.11	1.37	3.08
	3-3	1.01	1.25	2.81
	3-4	1.21	1.49	3.35

Based on the values of fracture toughness obtained we see that the rock with highest value is the amphibolite of borehole KFM01D (1.93 ± 0.14 MPa m$^{1/2}$) while the lowest one is that corresponding to the albitized granodiorite of borehole KFM09B. The samples of the two different depths of borehole KFM08C display intermediate values, with the maximum value in this case corresponding to the albitized granodiorite (1.17 ± 0.08 MPa m$^{1/2}$) and the minimum to the amphibolite (1.00 ± 0.10 MPa m$^{1/2}$).

Table 3-4 and Table 3-5 summarize also the results of the measurements of ultrasonic wave propagation velocities as well as the derived dynamic elastic moduli. We see that larger V_P are associated with the two amphibolites tested although this is not so clear in the case of V_S, for which the lowest values are associated with borehole KFM09B. Similar happens with the dynamic Young's, shear and bulk moduli, for which amphibolite rocks display greater values.

Table 3-3. Results of the fracture toughness tests.

Borehole	Specimen	P_{max} (N)	P_Q (N)	P_{max}/P_Q (–)	K_Q (MPa m$^{1/2}$)	$K_{Q,mean}$ (MPa m$^{1/2}$)	Rock Type
KFM08C	1-1	829	789	1.05	1.26		
	1-2	744	692	1.08	1.05	1.17 ± 0.08	101057_104
	1-3	819	787	1.04	1.31		
	1-4	683	672	1.02	1.06		
KFM08C	4-1	650	598	1.09	0.93		
	4-2	610	556	1.10	0.84	1.00 ± 0.10	102017
	4-3	704	643	1.09	0.98		
	4-4	855	791	1.08	1.26		
KFM01D	2-1	1122	1115	1.01	1.70		
	2-2	1101	1101	1.00	1.77	1.93 ± 0.14	102017
	2-3	1329	1392	0.95	2.21		
	2-4	1293	1293	1.00	2.04		
KFM09B	3-1	507	493	1.03	0.78		
	3-2	563	529	1.07	0.83	0.82 ± 0.02	101057_104
	3-3	542	509	1.07	0.79		
	3-4	605	559	1.08	0.87		

Notes: P_{max} = peak load at failure; P_Q = conditional load level; K_Q = conditional fracture toughness; $K_{Q,mean}$ = mean conditional fracture toughness ± standard error of the mean. Rock types 102017 and 101057_104 are amphibolite and albitized granodiorite, respectively

Table 3-4. Average values (± standard error of the mean) of the ultrasonic compressive (V$_P$) and shear (V$_S$) wave velocities, as well as their corresponding ratio.

Borehole	Adj Secup (m)	Adj Seclow (m)	V$_P$ (km/s)	V$_S$ (km/s)	V$_P$ / V$_S$ (–)	Rock Type
KFM08C	358,00	358,22	5.55 ± 0.13	3.11 ± 0.08	1.79 ± 0.01	101057_104
KFM08C	549,65	549,90	5.72 ± 0.16	3.02 ± 0.07	1.89 ± 0.03	102017
KFM01D	397,33	397,60	6.06 ± 0.03	3.39 ± 0.03	1.79 ± 0.02	102017
KFM09B	604,00	604,22	5.12 ± 0.14	2.62 ± 0.07	1.95 ± 0.02	101057_104

Note: Rock types 102017 and 101057_104 are amphibolite and albitized granodiorite, respectively

Table 3-5. Average values (± standard error of the mean) of the elastic dynamic moduli of the tested rocks.

Borehole	Adj Secup (m)	Adj Seclow (m)	E$_{dyn}$ (GPa)	ν$_{dyn}$ (GPa)	G$_{dyn}$ (GPa)	K$_{dyn}$ (GPa)
KFM08C	358,00	358,22	64.14 ± 2.83	0.27 ± 0.00	25.23 ± 1.12	46.75 ± 20.6
KFM08C	549,65	549,90	70.51 ± 3.04	0.31 ± 0.01	27.01 ± 1.15	60.70 ± 3.82
KFM01D	397,33	397,60	85.72 ± 1.00	0.27 ± 0.01	33.72 ± 0.58	62.70 ± 1.63
KFM09B	604,00	604,22	47.73 ± 2.22	0.32 ± 0.00	18.06 ± 0.86	44.69 ± 2.04

Notes: E$_{dyn}$ = dynamic Young's modulus; ν$_{dyn}$ = dynamic Poisson's ratio; G$_{dyn}$ = dynamic shear modulus; K$_{dyn}$ = dynamic bulk modulus

References

SKB's (Svensk Kärnbränslehantering AB) publications can be found at www.skb.com/publications.

ASTM, 2005. Standard test method for laboratory determination of pulse velocities and ultrasonic elastic constants of rock, D2845-05. Book of Standards Volume 4.08. ASTM International. West Conshohocken, PA. 7 p. (doi: 10.1520/D2845-05)

ASTM, 2012. Standard test method for linear-elastic plane-strain fracture toughness KIc of metallic material, E399-12. Book of Standards Volume 03.01. ASTM International. West Conshohocken, PA. 33 p. (doi: 10.1520/E0399-12)

Aydin A, 2014. Upgraded ISRM suggested method for determining sound velocity by ultrasonic pulse transmission technique. Rock Mechanics and Rock Engineering 47, 255–259. (doi: 10.1007/s00603-013-0454-z)

Delgado-Martin J, Muñoz-Ibáñez A, Herbón-Penabad M, Alejano L R, 2021. Fracture toughness using pseudo-compact tension (*p*CT) test and semi-circular bending specimen (SCB) test. SKB P-21-02, Svensk Kärnbränslehantering AB.

Dutler N, Nejati M, Valley B, Amann F, Molinari G, 2018. On the link between fracture toughness, tensile strength, and fracture process zone in anisotropic rocks. Engineering Fracture Mechanics 201, 56–79. (doi: 10.1016/j.engfracmech.2018.08.017)

ISRM, 1988. Suggested methods for determining the fracture toughness of rock. International Journal of Rock Mechanics and Mining Sciences & Geomechanical Abstracts 25(2), 71–96 (doi: 10.1016/0148-9062(88)91871-2)

Kuruppu M D, Obara Y, Ayatollahi M R, Chong K P, Funatsu T, 2014. ISRM-suggested method for determining the mode I static fracture toughness using semi-circular bend specimen. Rock Mechanics and Rock Engineering 47, 267–274 (doi: 10.1007/s00603-013-0422-7)

Maeda N, 1985. A method for reading and checking phase time in auto-processing system of seismic wave data. Journal of the Seismological Society of Japan 60, 365–379 (doi: 10.4294/ZISIN1948.38.3_365)

Muñoz-Ibáñez A, Delgado-Martín J, Costas M, Rabuñal-Dopico J, Alvarellos-Iglesias J, Canal-Vila J, 2020. Pure mode-I fracture toughness determination in rocks using a pseudo-compact tension (*p*CT) test approach. Rock Mechanics and Rock Engineering 53, 3267–3285 (doi: 10.1007/s00603-020-02102-6)

Muñoz-Ibáñez A, Delgado-Martín J, Juncosa-Rivera R, 2021. Size effect and other effects on mode I fracture toughness using two testing methods. International Journal of Rock Mechanics and Mining Engineering 143, 104785 (doi: 10.1016/j.ijrmms.2021.104785)

Stephens M B, Fox A, La Pointe P, Simeonov A, Isaksson H, Hermanson J, Öhman J, 2007. Geology Forsmark. Site descriptive modelling Forsmark stage 2.2. SKB R-07-45, Svensk Kärnbränslehantering AB.

Waber H N, Smellie J A T, 2007. Forsmark site investigation. Boreholes KFM01D, KFM08C, KFM09B. Characterisation of pore water. Part 1 Diffusion experiments and pore-water data. SKB P-07-119, Svensk Kärnbränslehantering AB.

Appendix 1

Ultrasonic Wave Velocities and Derived Data

Table A1-1. Identification of samples used in the ultrasonic velocity tests and their corresponding dimensions.

Borehole	Rock Type	Specimen	L_{mean} (mm)	D_{mean} (mm)	L/D (–)	M (g)	ρ (kg/m^3)
KFM08C	101057_104	1-1	25.87	50.94	0.51	137.98	2617
		1-2	27.05	50.88	0.53	142.47	2590
		1-3	25.62	50.98	0.50	135.95	2599
		1-4	26.20	50.99	0.51	139.81	2613
KFM08C	102017	4-1	27.13	50.78	0.53	160.52	2921
		4-2	27.05	50.79	0.53	161.33	2944
		4-3	26.90	50.77	0.53	162.36	2982
		4-4	26.69	50.92	0.52	161.39	2970
KFM01D	102017	2-1	27.30	50.39	0.54	158.58	2912
		2-2	26.19	50.41	0.52	153.02	2927
		2-3	26.45	50.51	0.52	155.60	2935
		2-4	26.59	50.44	0.53	156.00	2936
KFM09B	101057_104	3-1	27.01	50.91	0.53	143.39	2608
		3-2	26.36	50.91	0.52	140.75	2624
		3-3	26.45	50.94	0.52	141.30	2621
		3-4	26.45	50.94	0.52	141.28	2621

Notes: L_{mean} = mean length; D_{mean} = mean diameter; **L/D** = length-to-diameter ratio; **M** = mass of the samples after 7-days immersion in tap water; ρ = bulk density

Table A1-2. Ultrasonic velocity test results.

Borehole	Rock Type	Specimen	V_P (km/s)	V_{S1} (km/s)	V_{S2} (km/s)	V_S (km/s)	V_P/V_S (–)
KFM08C	101057_104	1-1	5.561	2.959	3.198	3.078	1.807
		1-2	5.442	2.958	3.166	3.062	1.777
		1-3	5.333	2.909	3.087	2.998	1.779
		1-4	5.868	3.255	3.346	3.301	1.778
KFM08C	102017	4-1	5.315	2.918	2.918	2.918	1.822
		4-2	5.798	2.956	2.937	2.946	1.968
		4-3	5.783	3.026	3.067	3.046	1.898
		4-4	5.964	3.200	3.151	3.175	1.878
KFM01D	102017	2-1	6.005	3.358	3.537	3.448	1.742
		2-2	6.126	3.269	3.370	3.320	1.845
		2-3	6.088	3.467	3.409	3.438	1.771
		2-4	6.036	3.370	3.366	3.368	1.792
KFM09B	101057_104	3-1	5.386	2.745	2.849	2.797	1.926
		3-2	5.225	2.617	2.617	2.617	1.996
		3-3	5.024	2.571	2.604	2.587	1.942
		3-4	4.849	2.510	2.479	2.494	1.944

Notes: V_P= compressional velocity; V_{S1}= shear velocity; V_{S2}= shear velocity at 90° of V_{S1}; V_S = average shear velocity

Table A1-3. Ultrasonic velocity test results. Dynamic moduli.

Borehole	Rock Type	Specimen	E_{dyn} (GPa)	ν_{dyn} (–)	G_{dyn} (GPa)	K_{dyn} (GPa)
KFM08C	101057_104	1-1	63.46	0.28	24.80	47.88
		1-2	61.61	0.27	24.29	44.32
		1-3	59.28	0.27	23.36	42.77
		1-4	72.24	0.27	28.47	52.04
KFM08C	102017	4-1	63.87	0.28	24.87	49.37
		4-2	67.78	0.33	25.56	64.89
		4-3	72.40	0.31	27.67	62.84
		4-4	77.99	0.30	29.95	65.70
KFM01D	102017	2-1	86.82	0.25	34.61	58.85
		2-2	83.37	0.29	32.26	66.83
		2-3	87.85	0.27	34.70	62.55
		2-4	84.85	0.27	33.30	62.57
KFM09B	101057_104	3-1	53.67	0.32	20.40	48.45
		3-2	47.90	0.33	17.97	47.65
		3-3	46.30	0.32	17.54	42.77
		3-4	43.05	0.32	16.31	39.88

Notes: E_{dyn}= dynamic Young's modulus; ν_{dyn} = dynamic Poisson's ratio; G_{dyn}= dynamic shear modulus; K_{dyn} = dynamic compressibility modulus

Appendix 2

Experimental Results

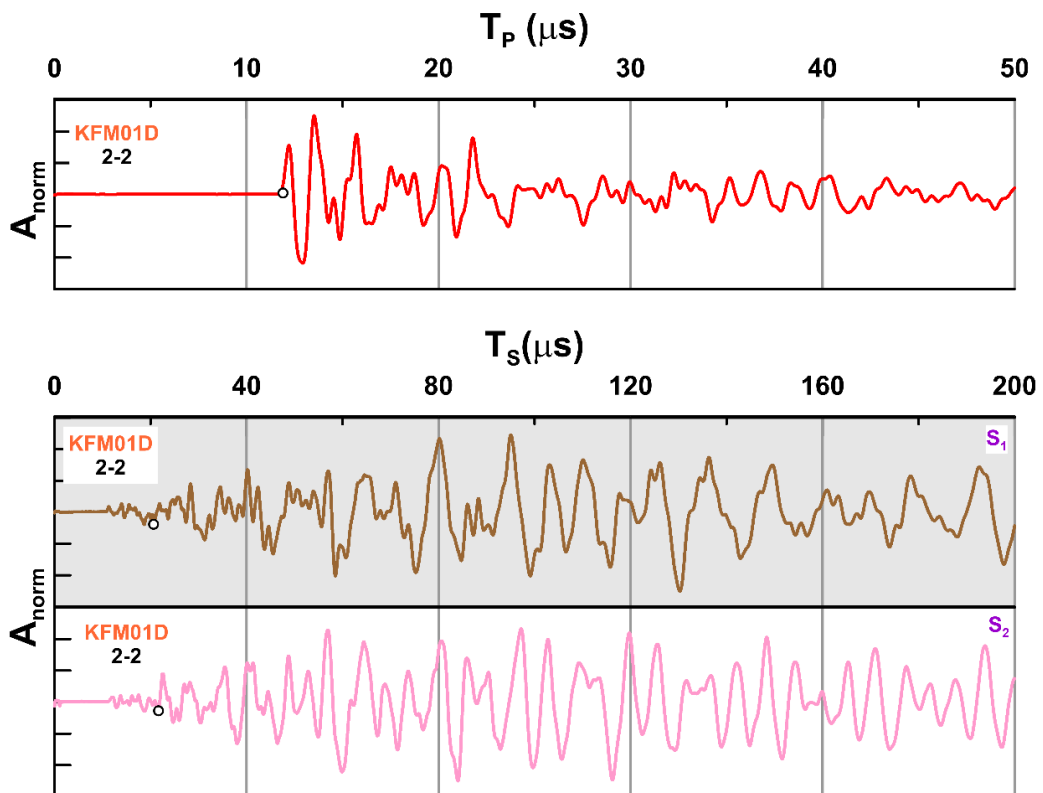*Figure A2-1.* *Measurement of ultrasonic velocities of sample KFM08C (1-1)*
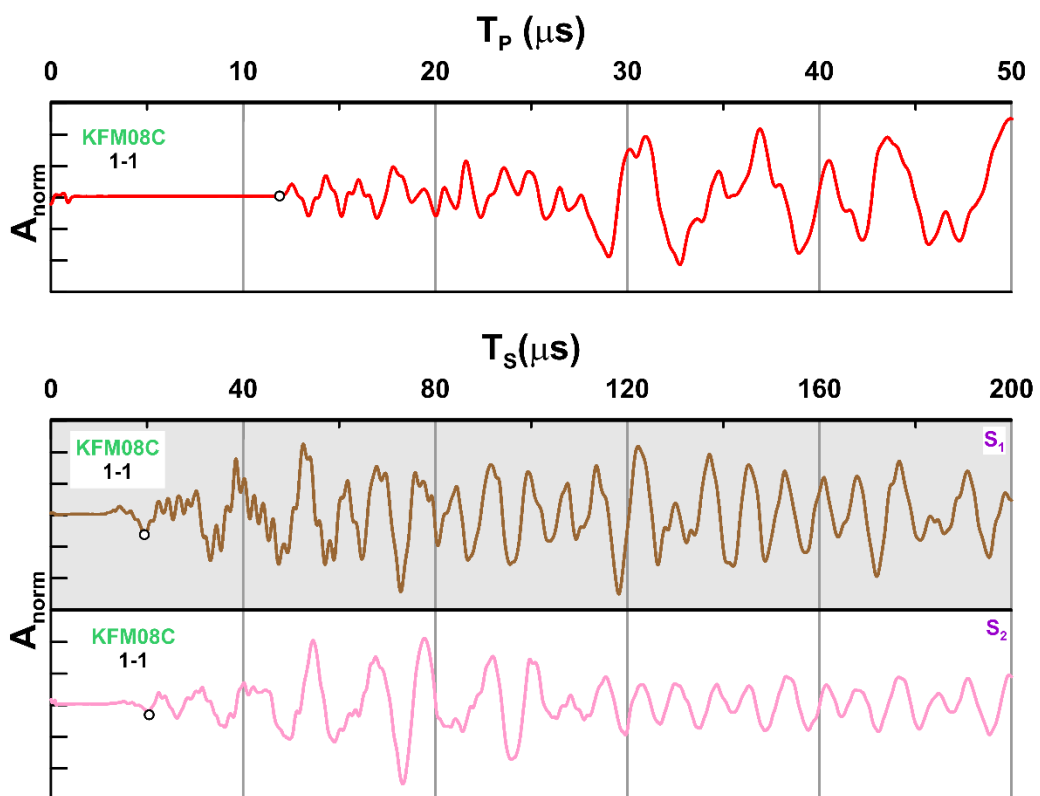
Figure A2-2. *Experimental results of ultrasonic wave velocities (UWV) performed with specimen 1-1*
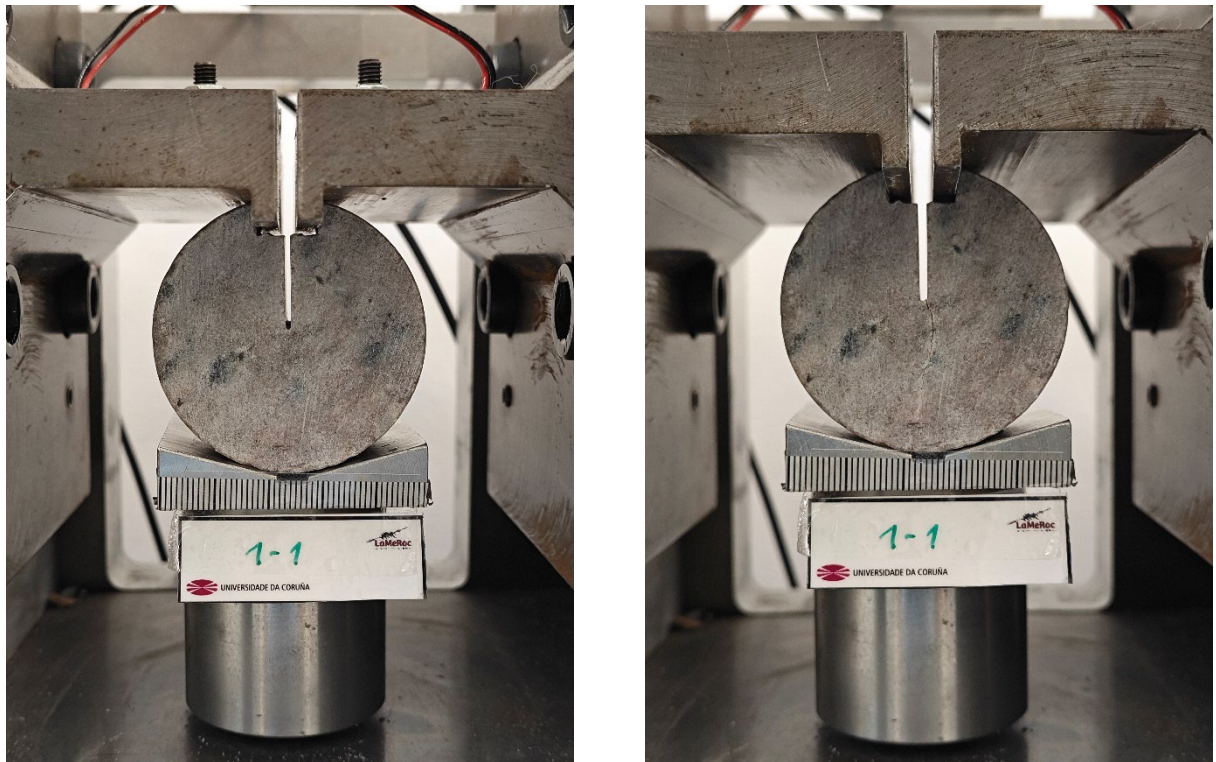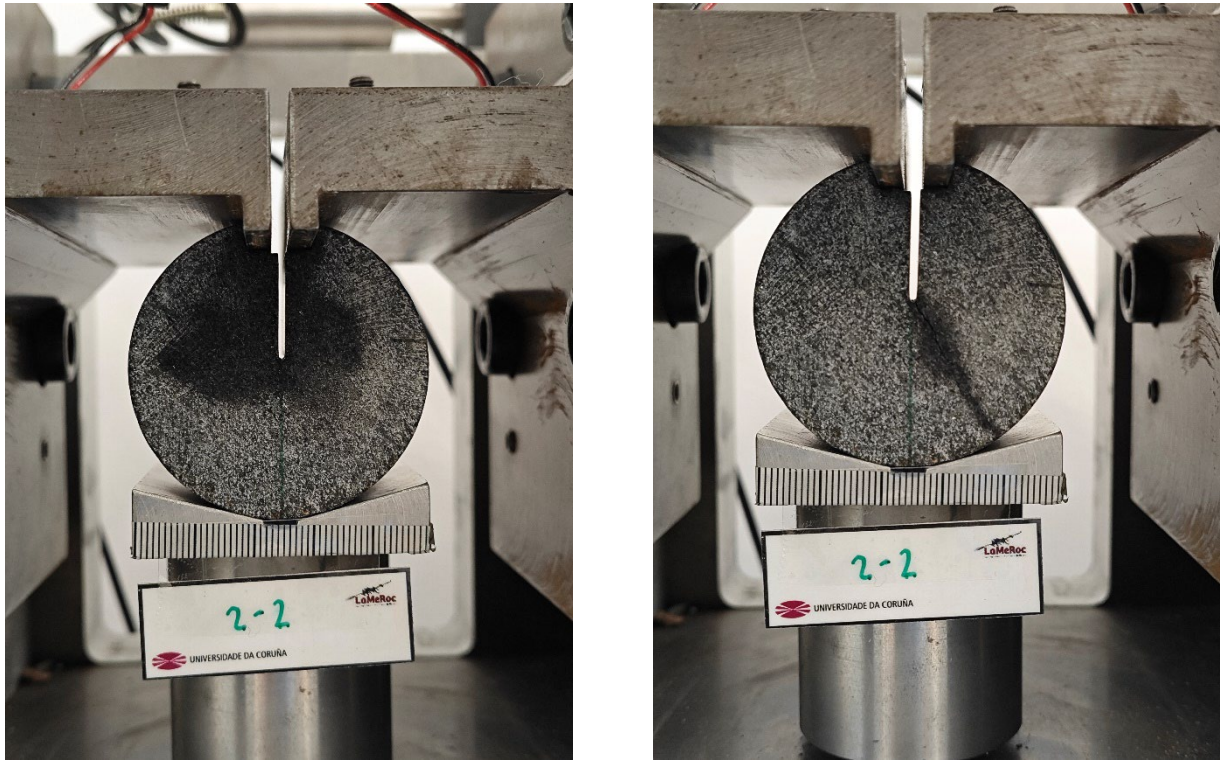
Figure A2-3. *Sample KFM08C (1-1) before (left) and after (right) the pCT test. The KIC value obtained was of 1.26 MPa m$^{1/2}$ obtained for a maximum load of 830 N*
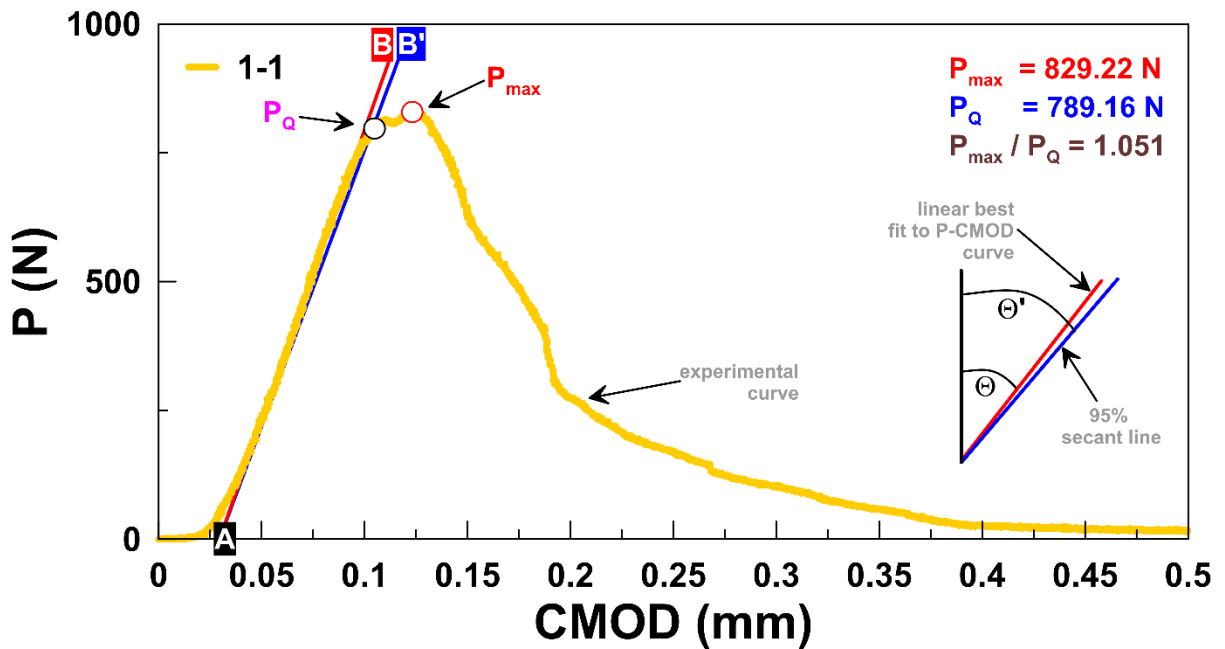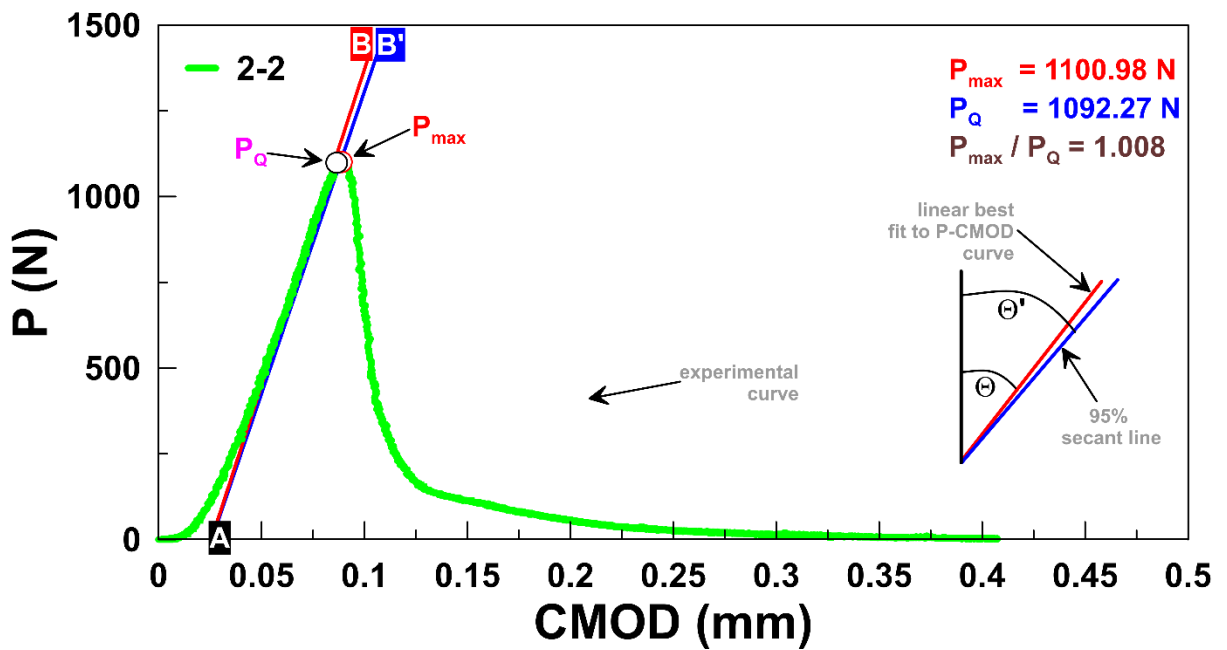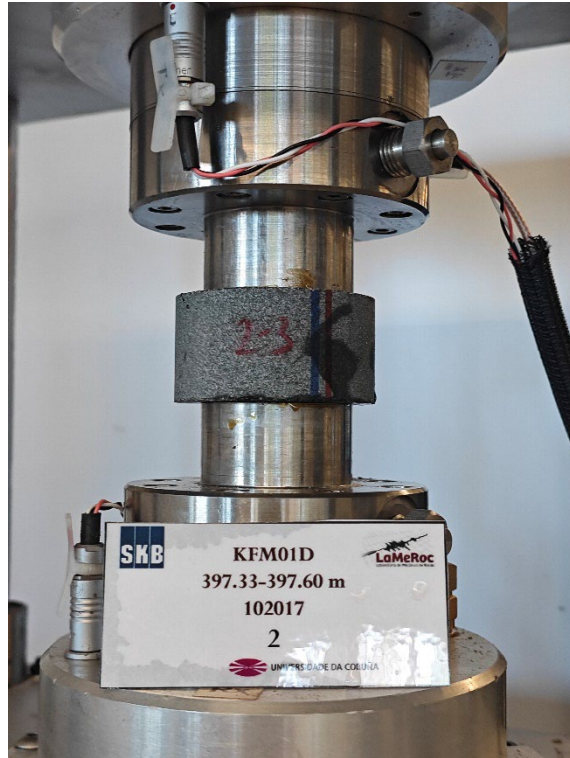

Figure A2-4. *Experimental results of the pCT test performed with specimen (1-1) and verification of the linearity criterion of the compliance method. See text for explanation.*

Notes: P = *applied horizontal load;* **P_{max}** = *maximum load;* **P_Q** = *conditional load;* **CMOD** = *crack mounth opening displacement (≡ load point displacement).*

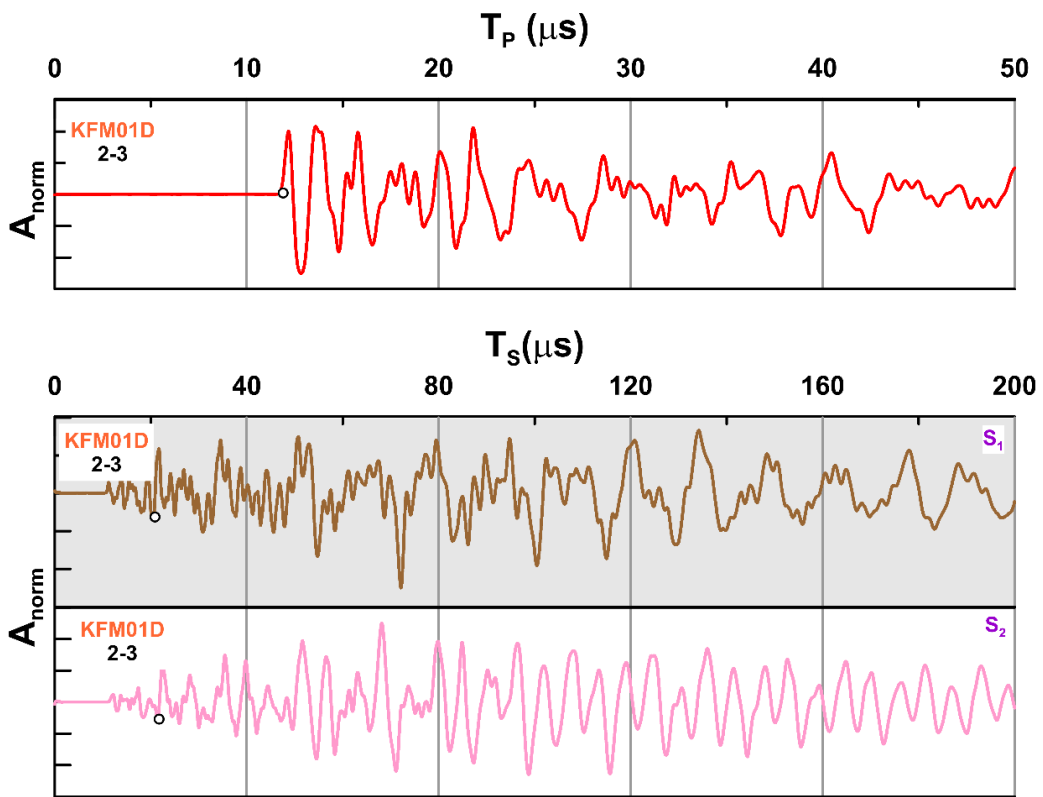***Figure A2-5.*** *Measurement of ultrasonic velocities of sample KFM08C (1-2)*
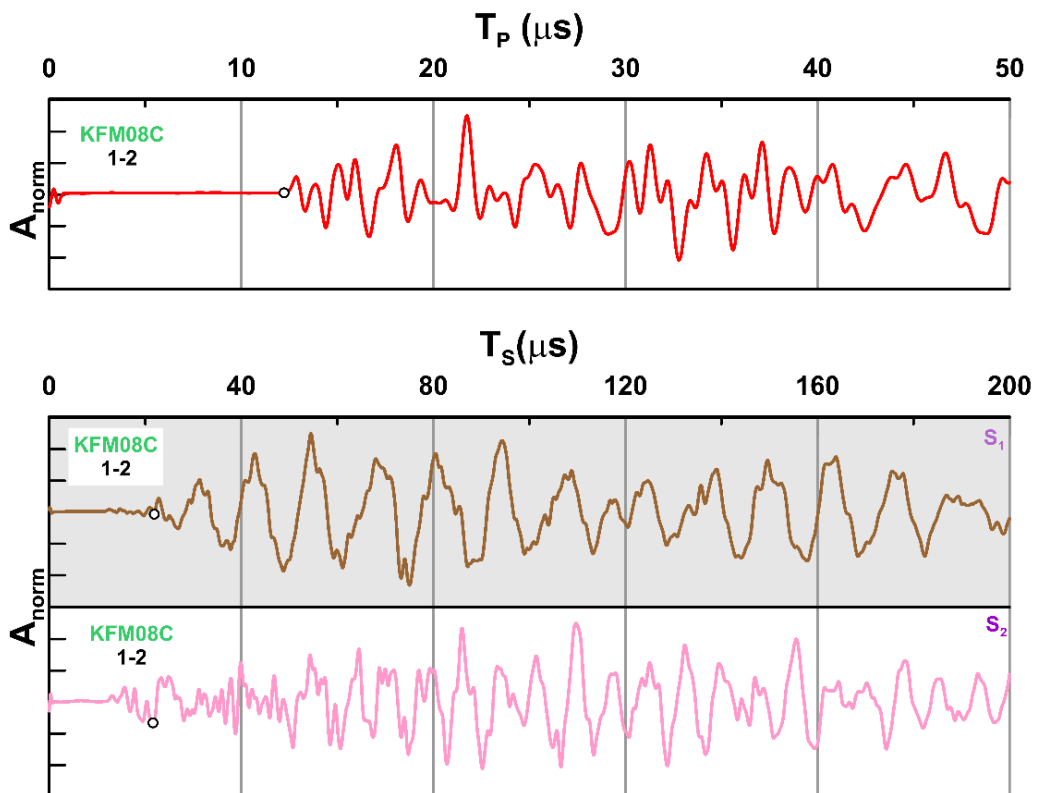
Figure A2-6. *Experimental results of ultrasonic wave velocities (UWV) performed with specimen 1-2*
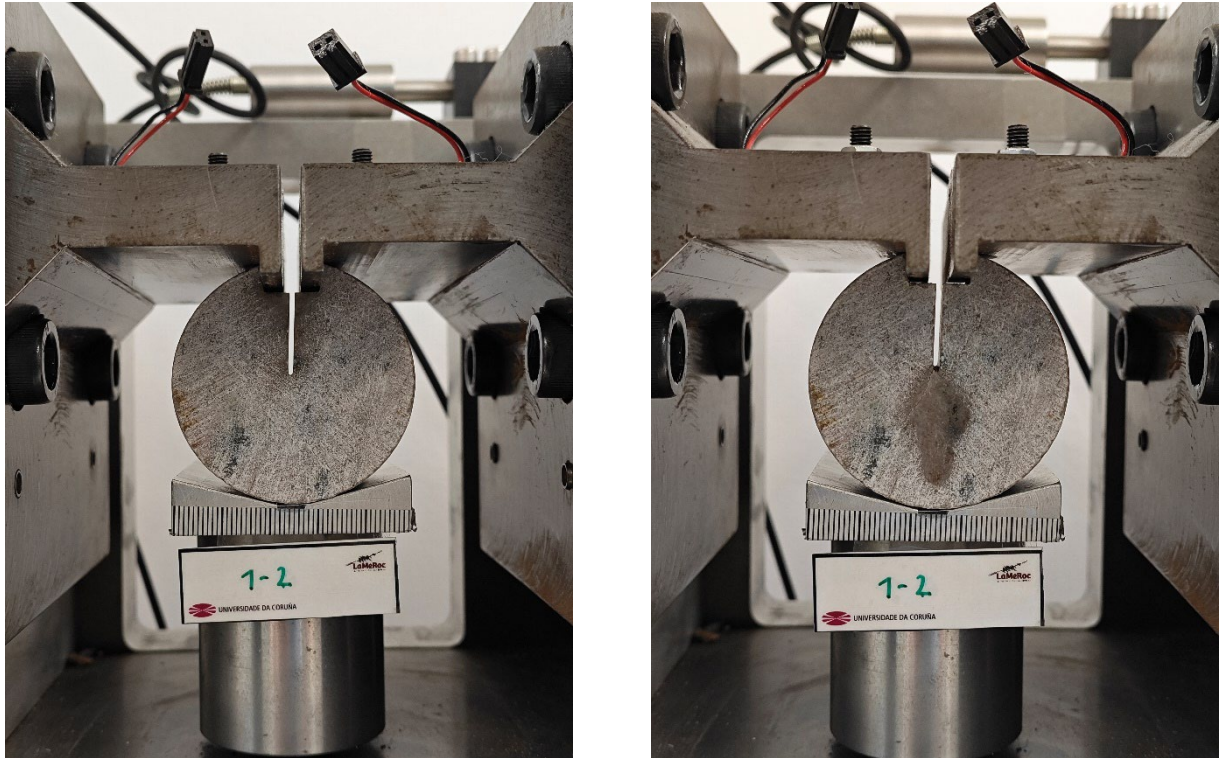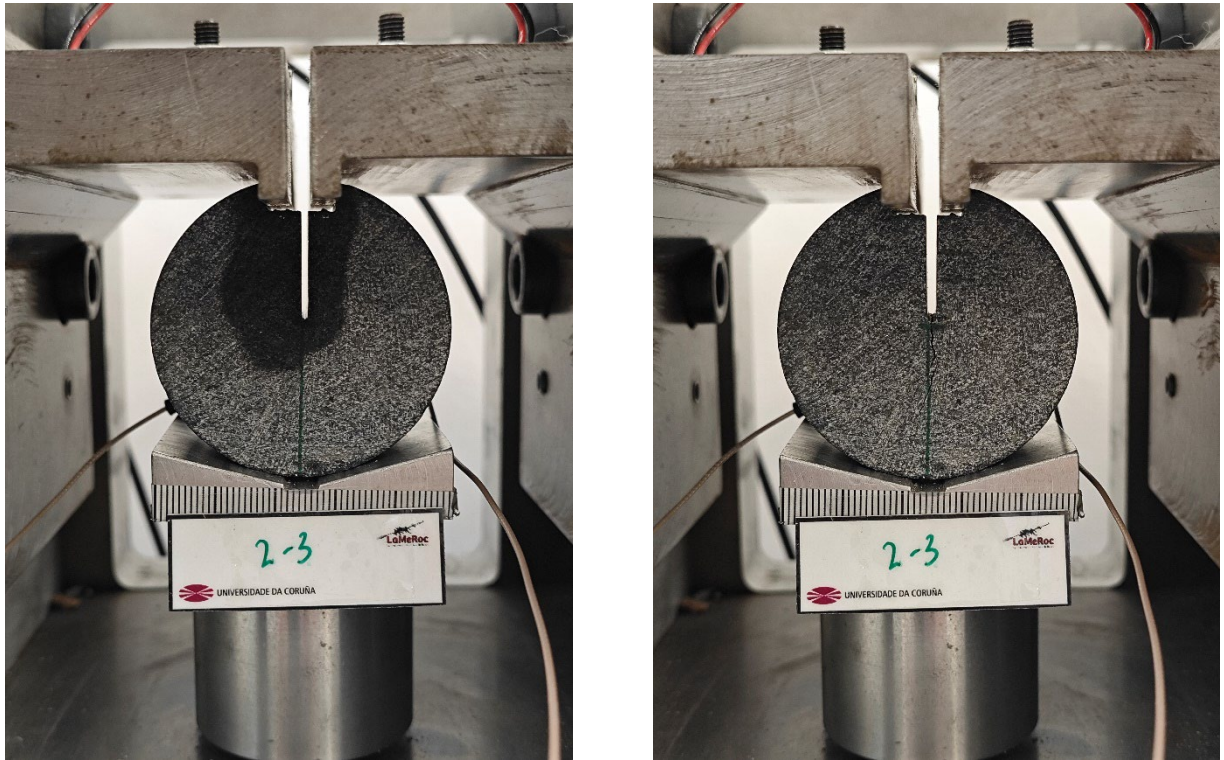
Figure A2-7. *Sample KFM08C (1-2) before (left) and after (right) the pCT test. The KIC value obtained was of 1.05 MPa m$^{1/2}$ obtained for a maximum load of 744 N*
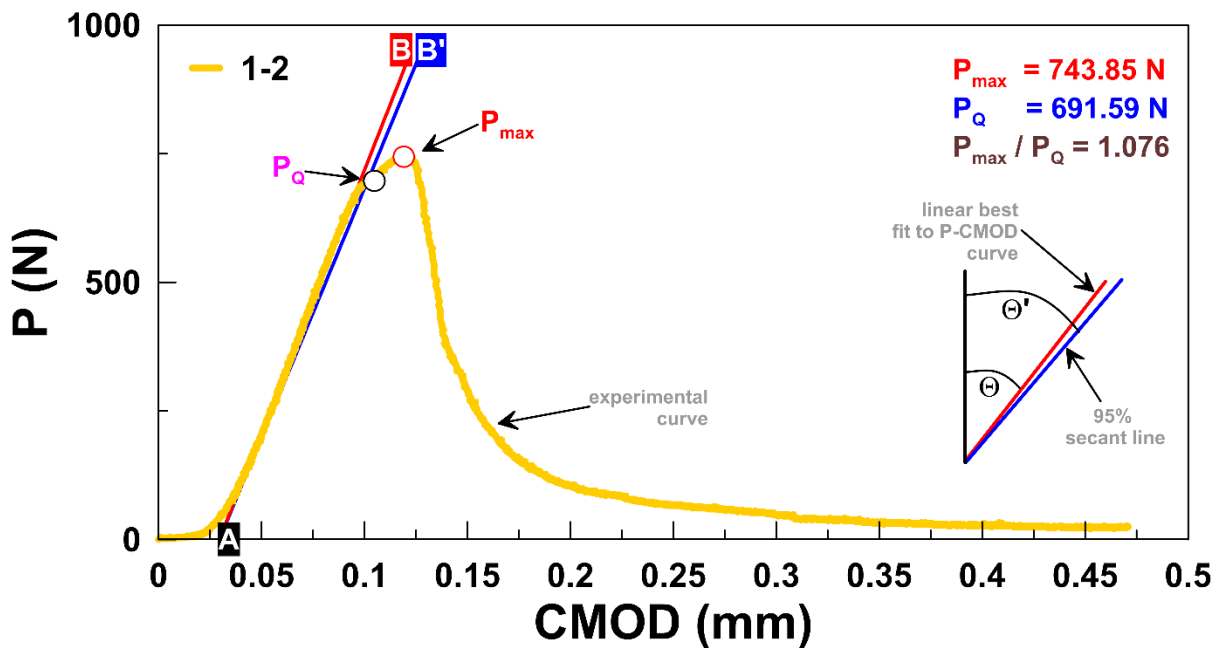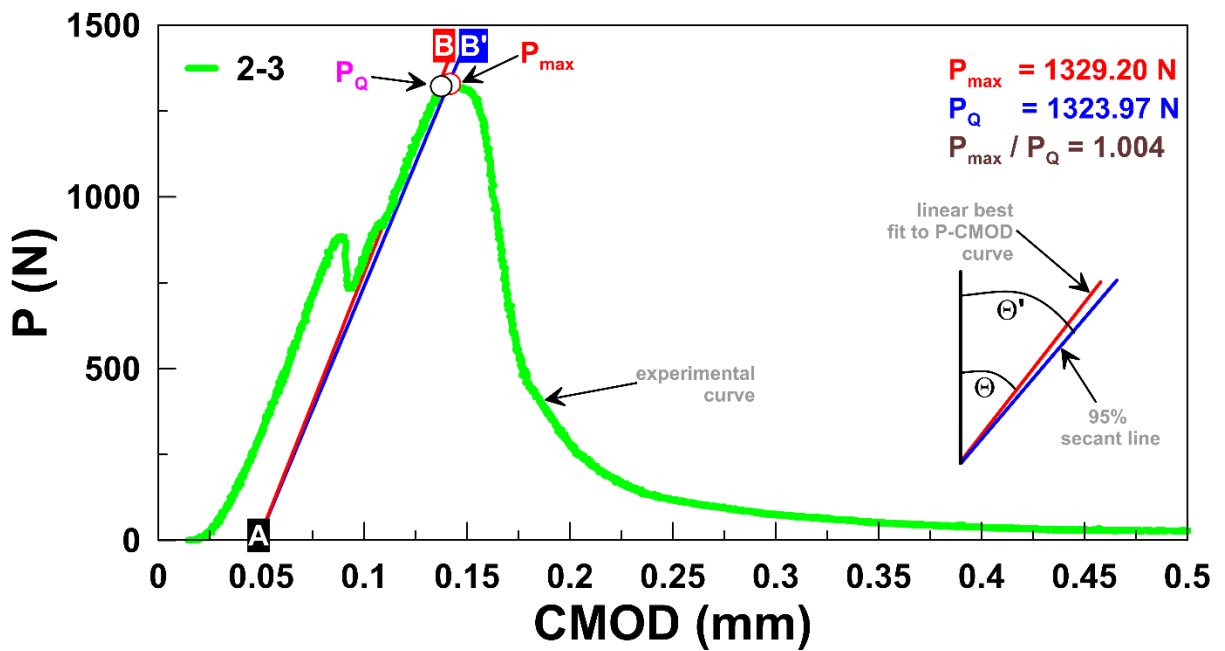

Figure A2-8. *Experimental results of the pCT test performed with specimen (1-2) and verification of the linearity criterion of the compliance method. See text for explanation.*

Notes: P = *applied horizontal load;* **P$_{max}$** = *maximum load;* **P$_Q$** = *conditional load;* **CMOD** = *crack mounth opening displacement (≡ load point displacement).*

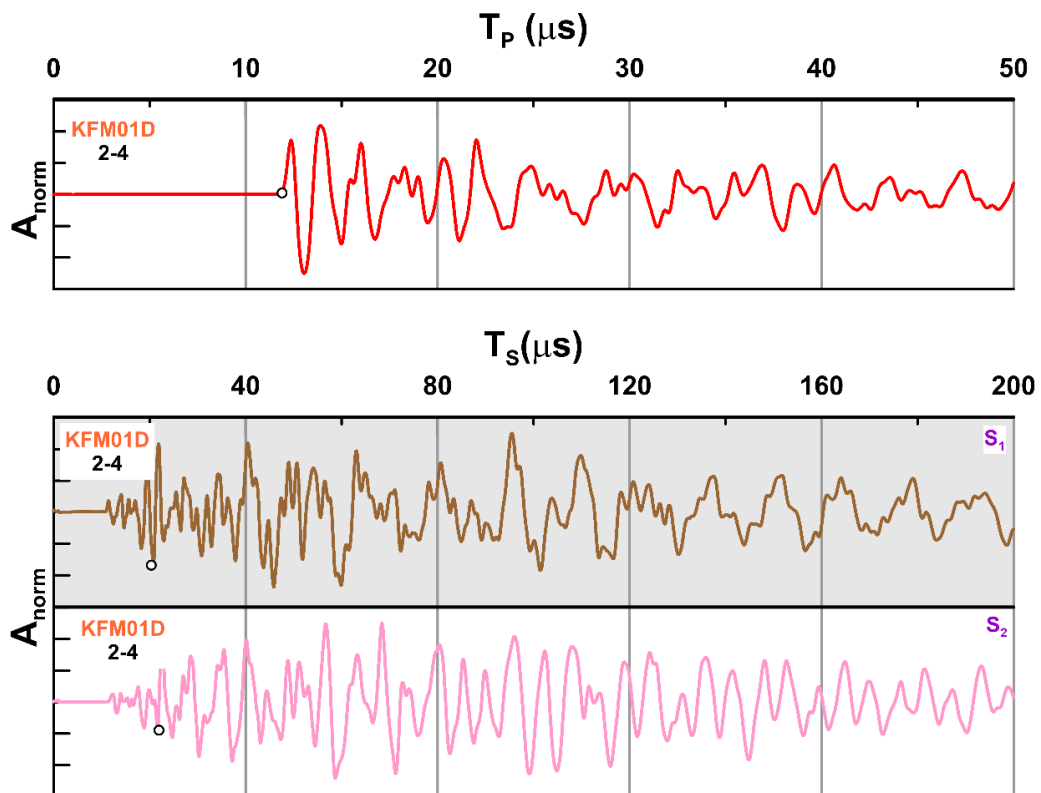*Figure A2-9. Measurement of ultrasonic velocities of sample KFM08C (1-3)*
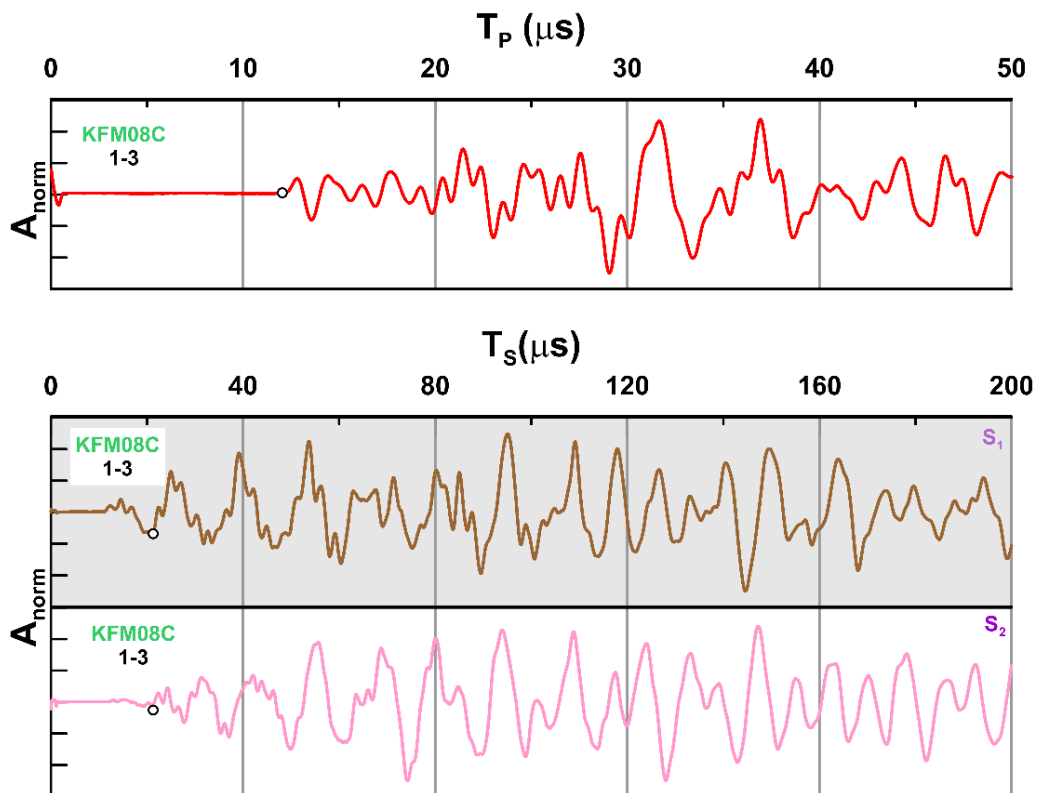
Figure A2-10. Experimental results of ultrasonic wave velocities (UWV) performed with specimen 1-3
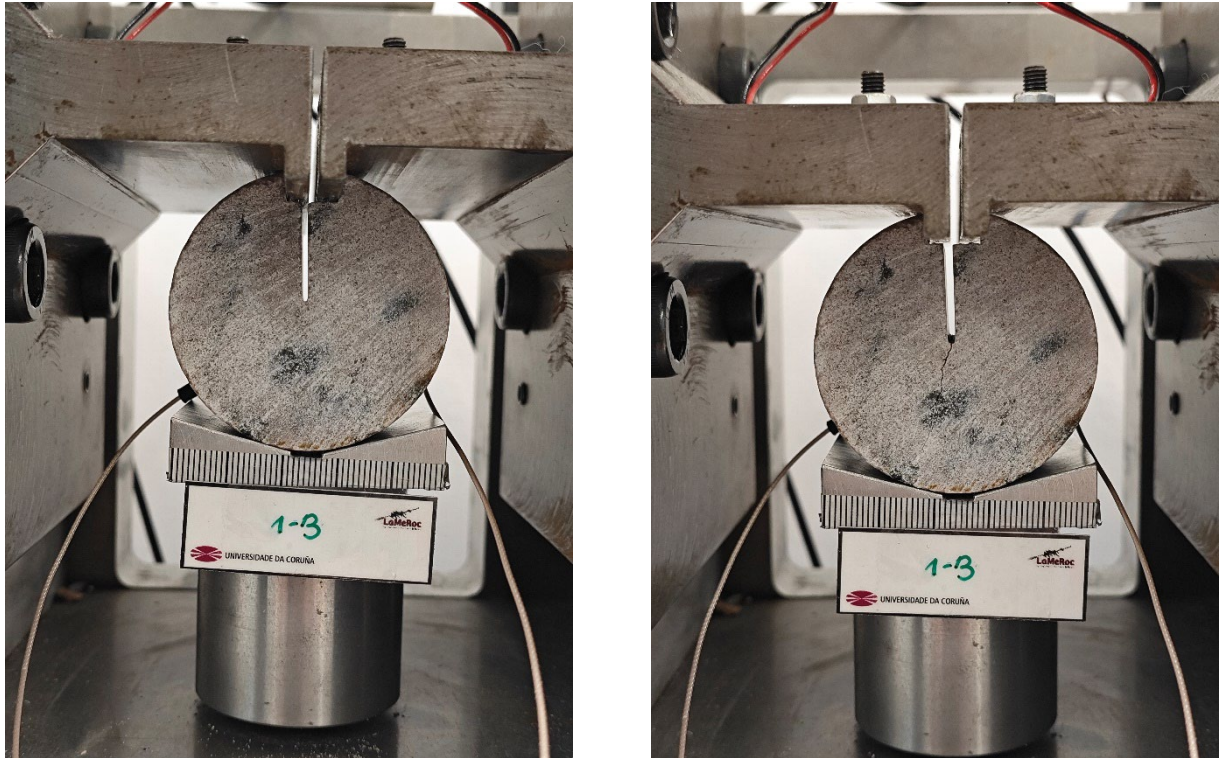
Figure A2-11. *Sample KFM08C (1-3) before (left) and after (right) the pCT test. The KIC value obtained was of 1.31 MPa m$^{1/2}$obtained for a maximum load of 819 N*
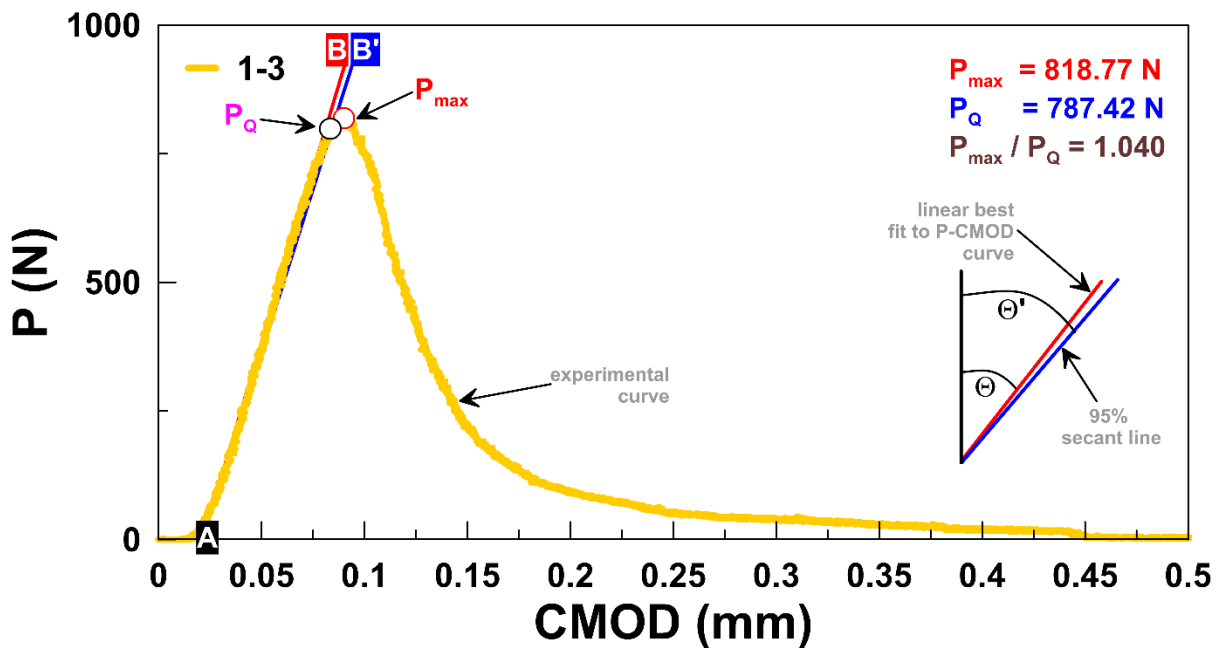
Figure A2-12. *Experimental results of the pCT test performed with specimen 1-3 and verification of the linearity criterion of the compliance method. See text for explanation.*

Notes: P *= applied horizontal load;* **P$_{max}$** *= maximum load;* **P$_Q$** *= conditional load;* **CMOD** *= crack mounth opening displacement (≡ load point displacement).*

Figure A2-13. *Measurement of ultrasonic velocities of sample KFM08C (1-4)*
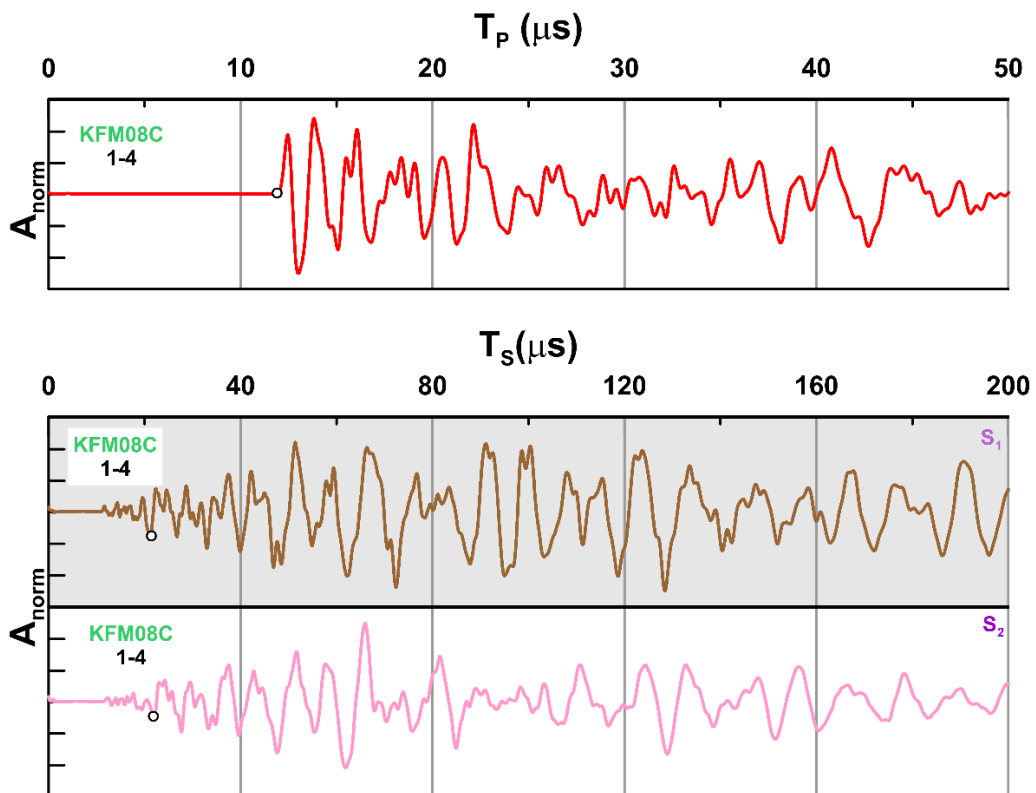
Figure A2-14. *Experimental results of ultrasonic wave velocities (UWV) performed with specimen 1-4*
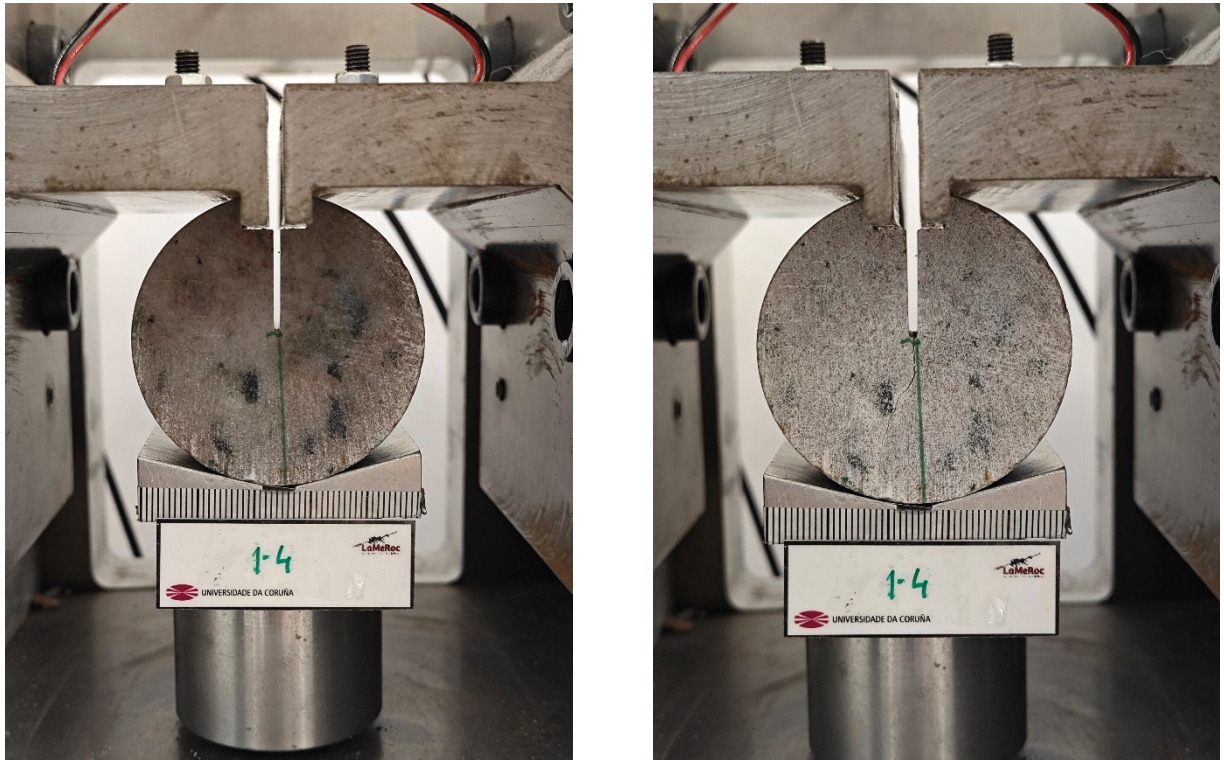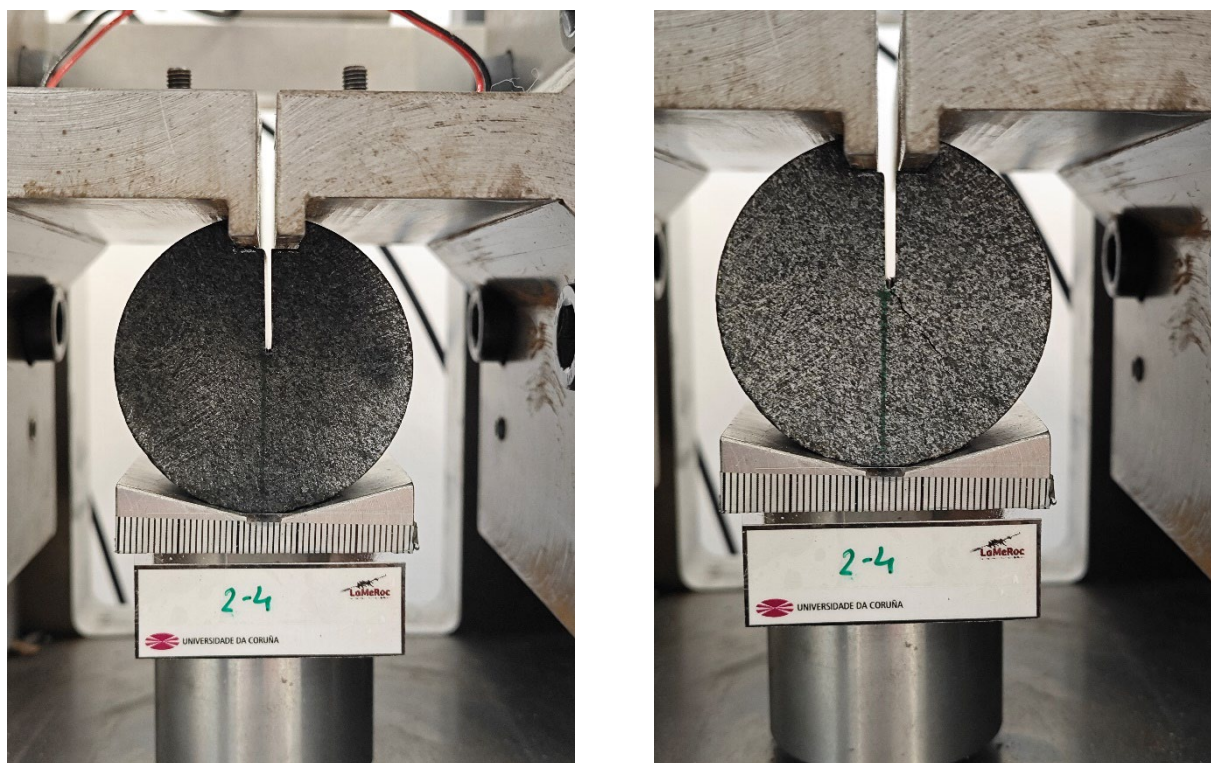
Figure A2-15. *Sample KFM08C 1-4 before (left) and after (right) the pCT test. The KIC value obtained was of 1.06 MPa m$^{1/2}$ obtained for a maximum load of 683 N*
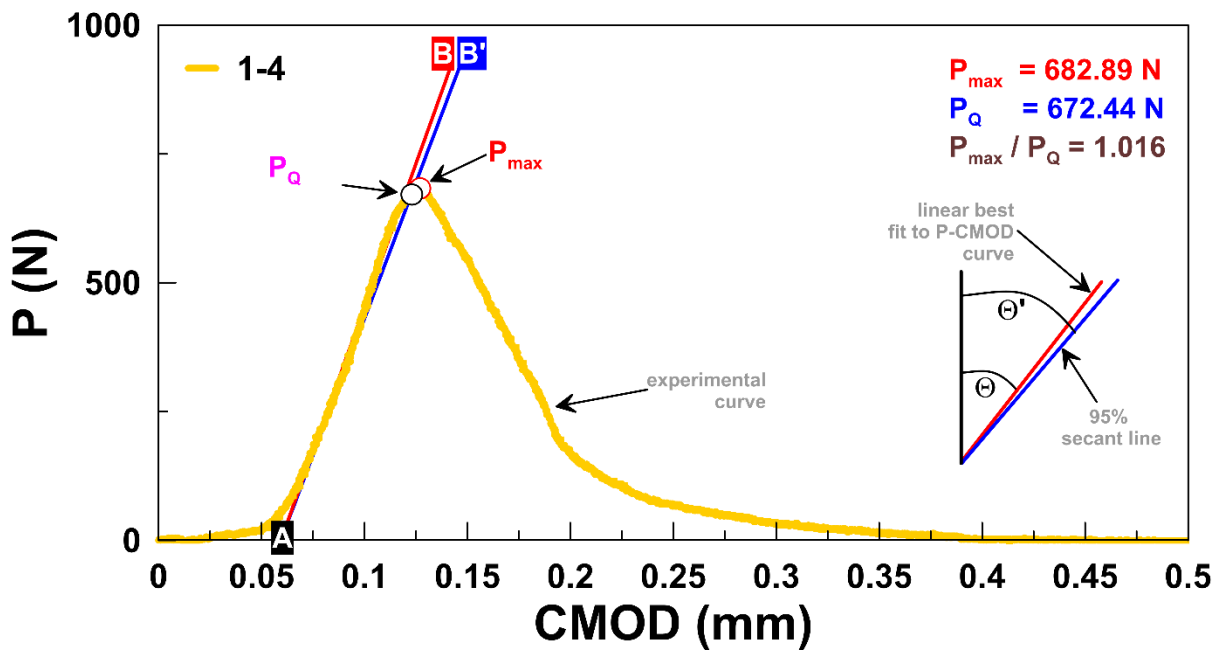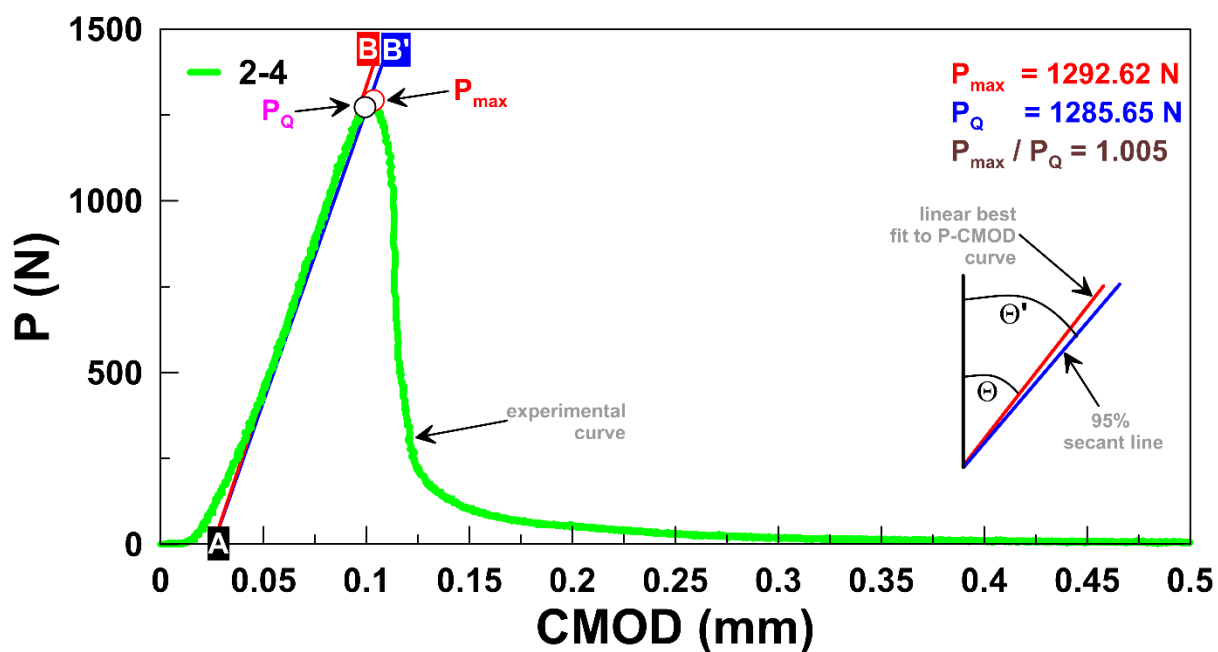

Figure A2-16. *Experimental results of the pCT test performed with specimen 1-4 and verification of the linearity criterion of the compliance method. See text for explanation.*

Notes: P = *applied horizontal load;* **P$_{max}$** = *maximum load;* **P$_Q$** = *conditional load;* **CMOD** = *crack mounth opening displacement (≡ load point displacement).*

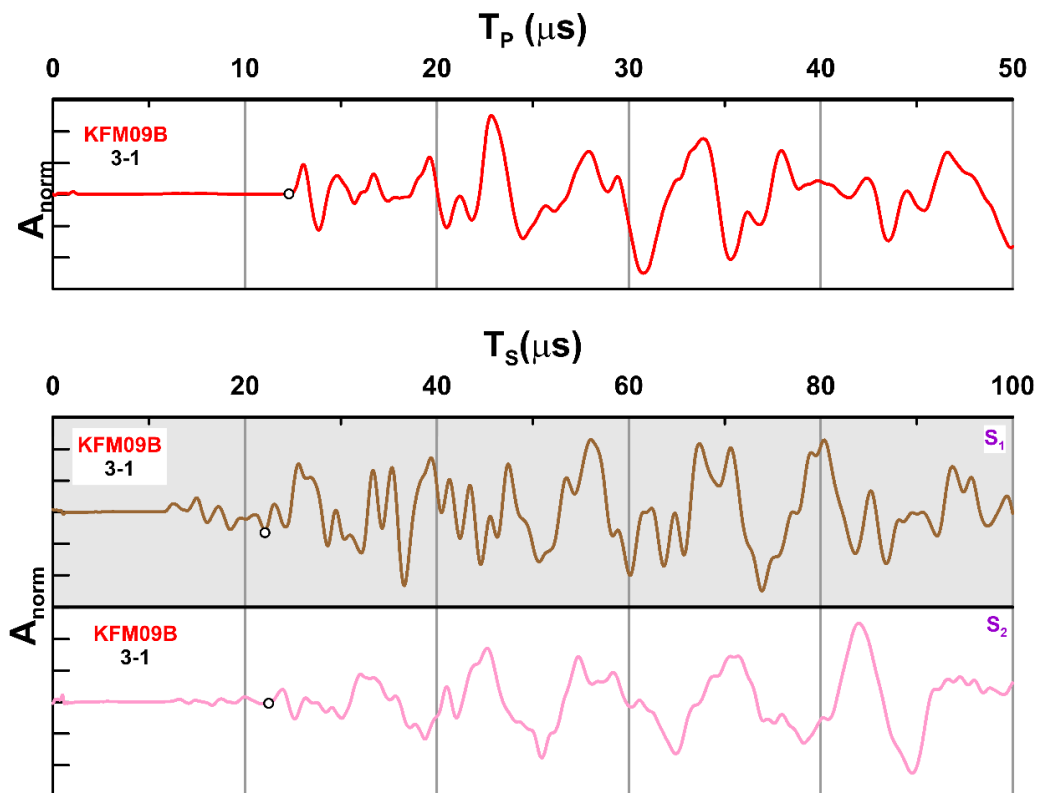**Figure A2-17.** *Measurement of ultrasonic velocities of sample KFM01D (2-1)*
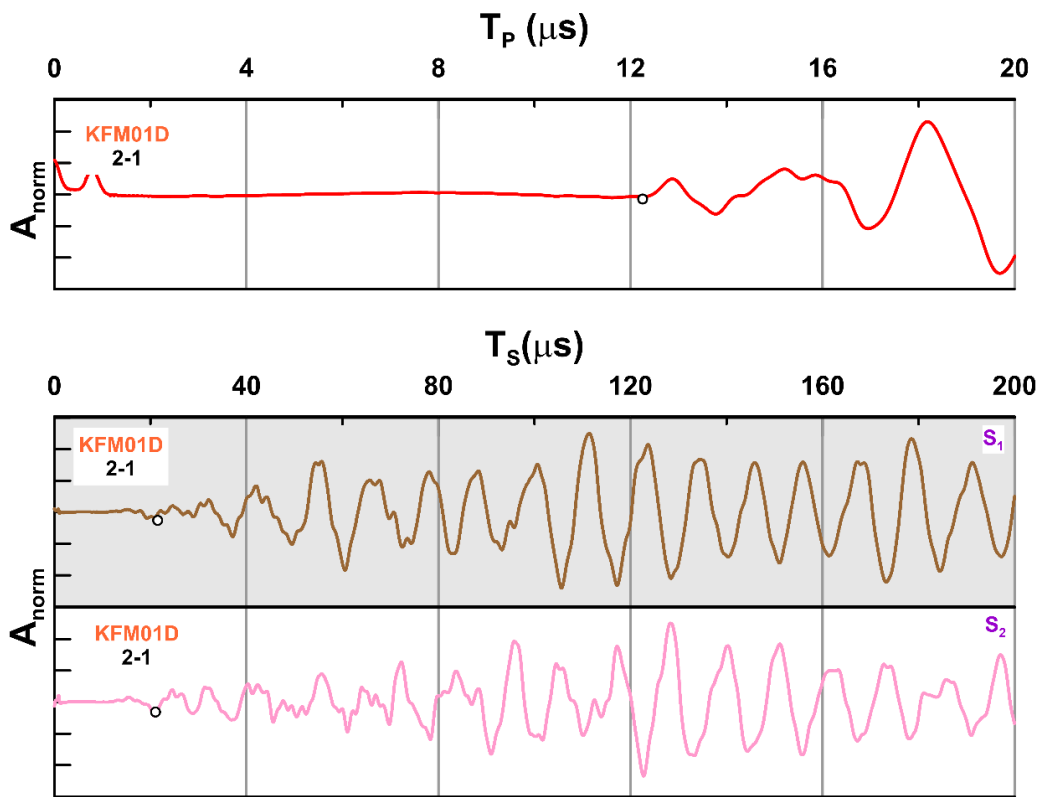
Figure A2-18. *Experimental results of ultrasonic wave velocities (UWV) performed with specimen 2-1*
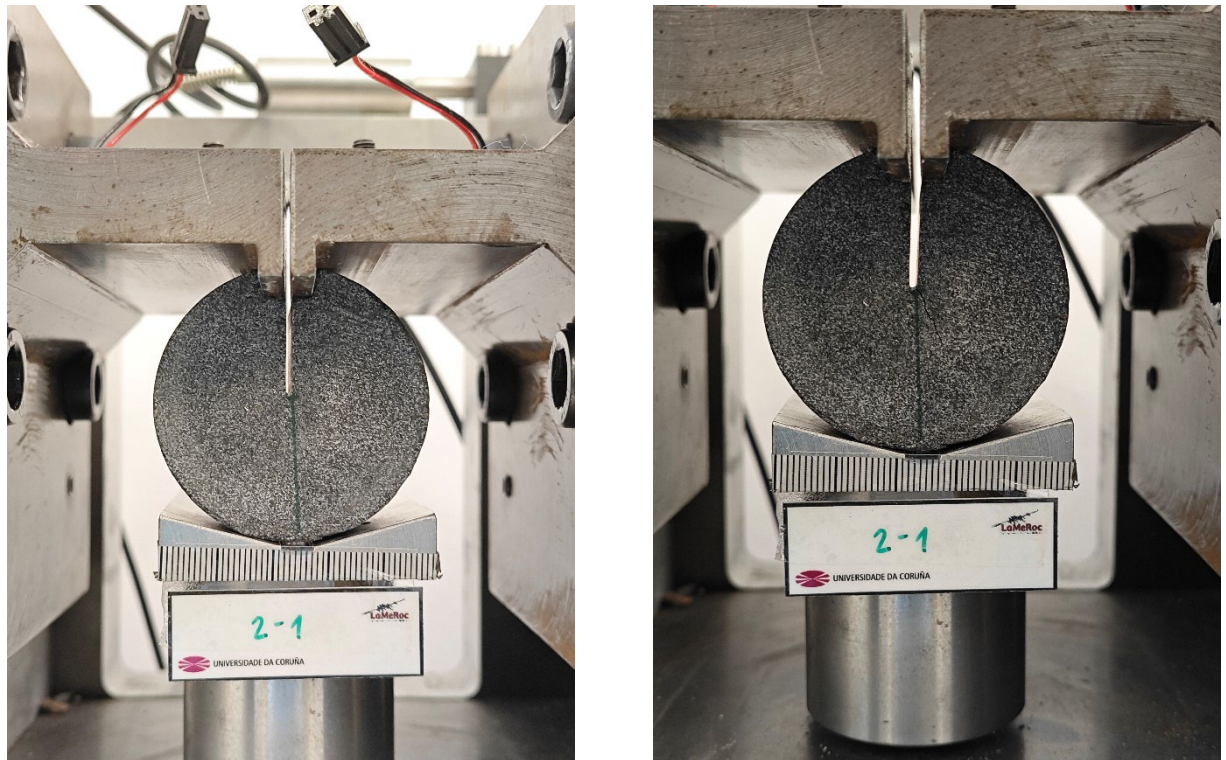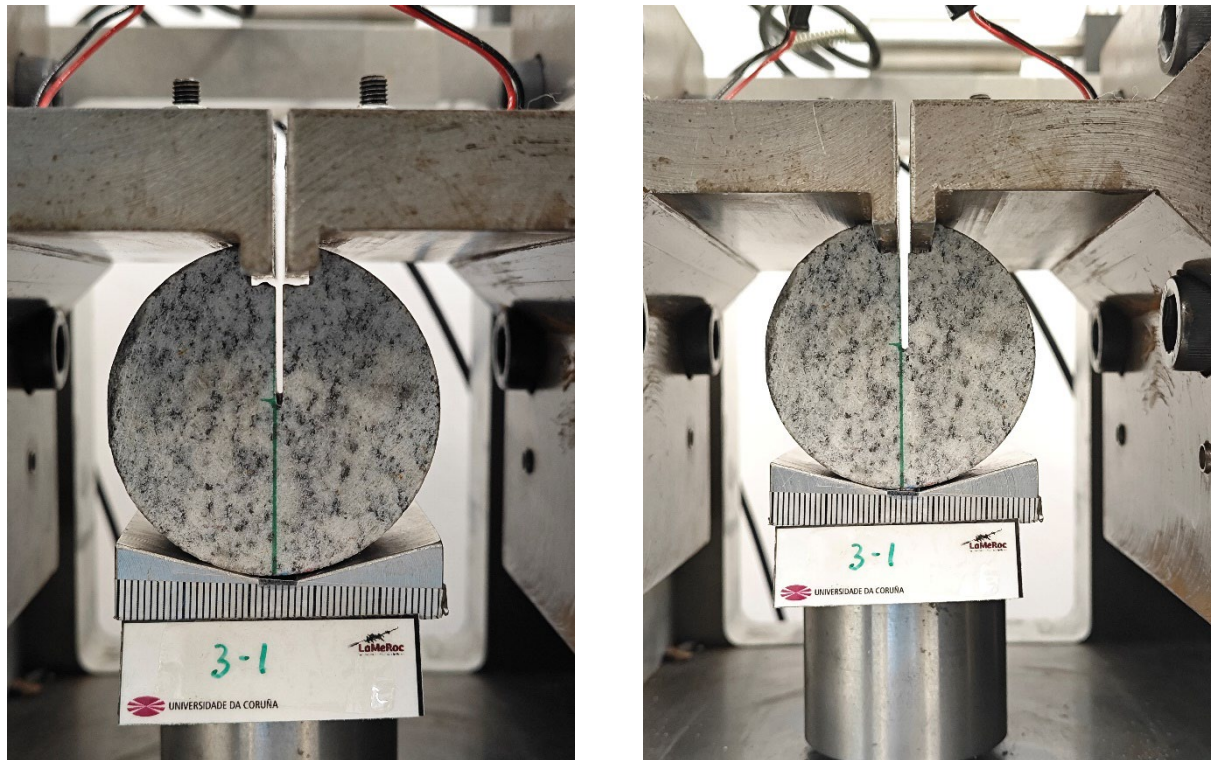
Figure A2-19. *Sample KFM01D 2-1 before (left) and after (right) the pCT test. The KIC value obtained was of 1.70 MPa m$^{1/2}$ obtained for a maximum load of 1122 N*
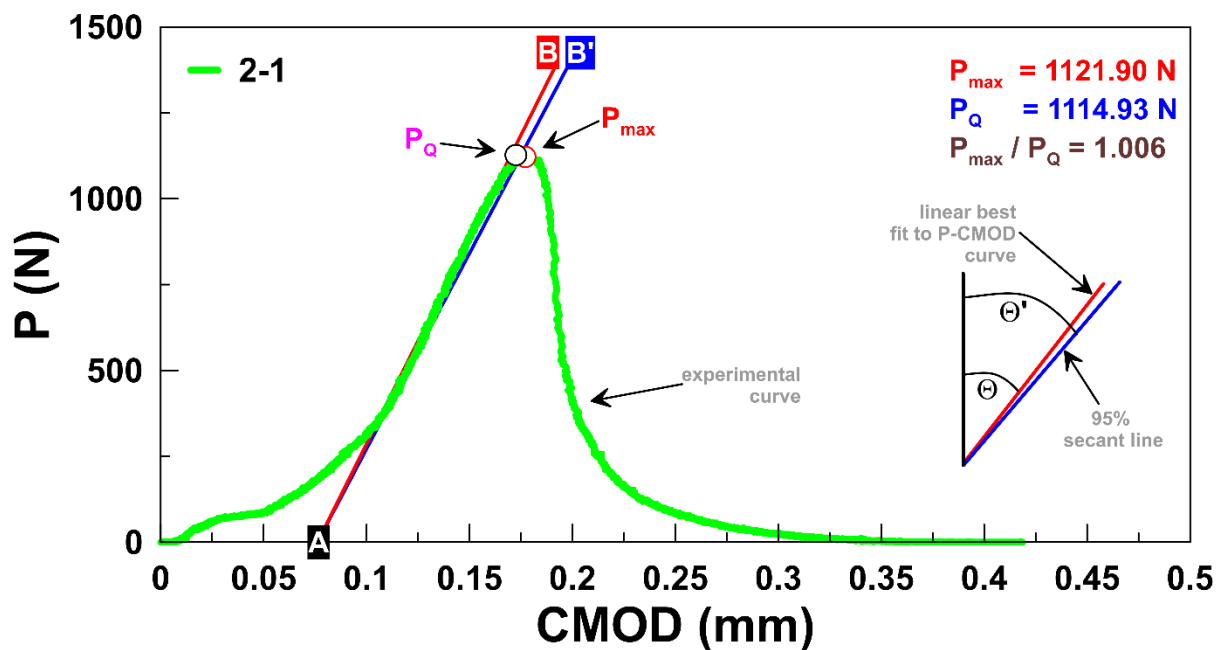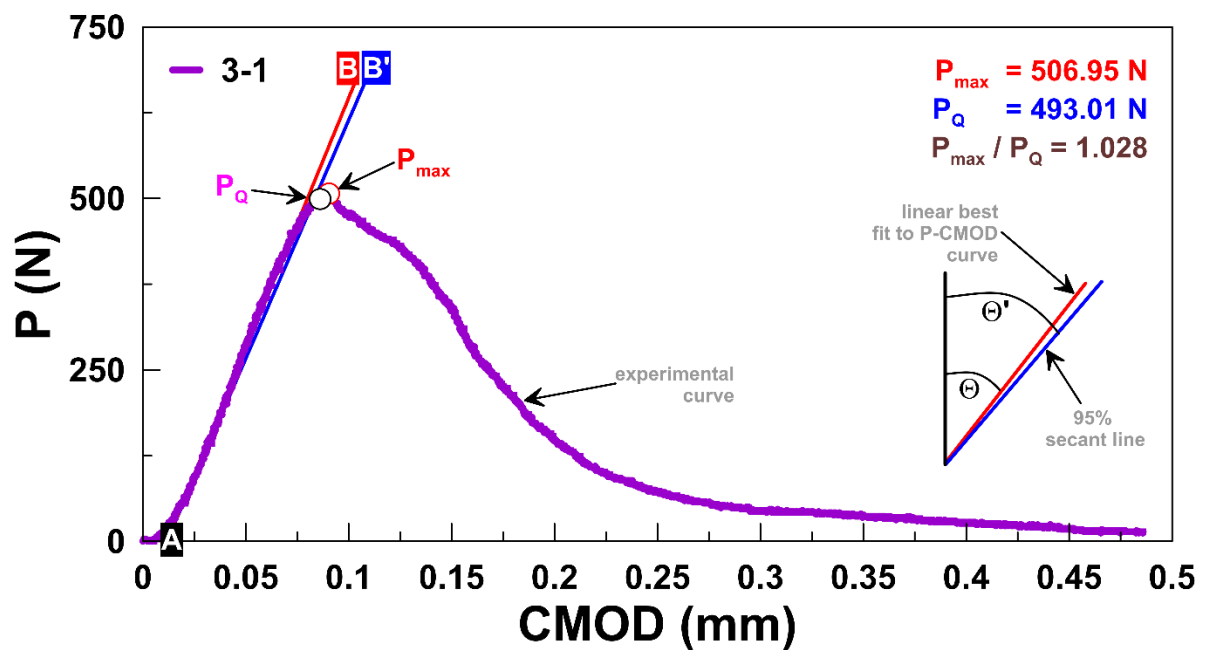

Figure A2-20. *Experimental results of the pCT test performed with specimen 2-1 and verification of the linearity criterion of the compliance method. See text for explanation.*

Notes: *P* *= applied horizontal load;* ***P$_{max}$*** *= maximum load;* ***P$_Q$*** *= conditional load;* ***CMOD*** *= crack mounth opening displacement (≡ load point displacement).*

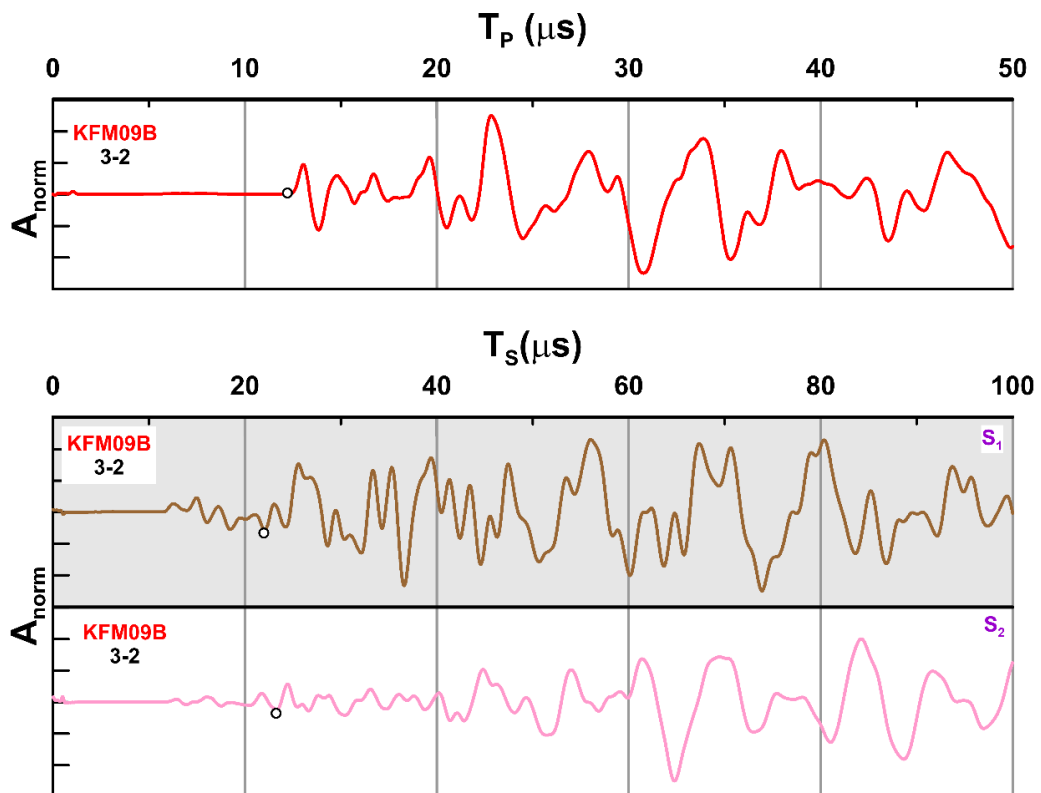**Figure A2-21.** *Measurement of ultrasonic velocities of sample KFM01D (2-2)*

Figure A2-22. *Experimental results of ultrasonic wave velocities (UWV) performed with specimen 2-2*

Figure A2-23. *Sample KFM01D 2-2 before (left) and after (right) the pCT test. The KIC value obtained was of 1.77 MPa m$^{1/2}$ obtained for a maximum load of 1101 N*

Figure A2-24. *Experimental results of the pCT test performed with specimen 2-2 and verification of the linearity criterion of the compliance method. See text for explanation.*

Notes: P = *applied horizontal load;* **P$_{max}$** = *maximum load;* **P$_Q$** = *conditional load;* **CMOD** = *crack mounth opening displacement (≡ load point displacement).*

Figure A2-25. *Measurement of ultrasonic velocities of sample KFM01D (2-3)*

Figure A2-26. *Experimental results of ultrasonic wave velocities (UWV) performed with specimen 2-3*
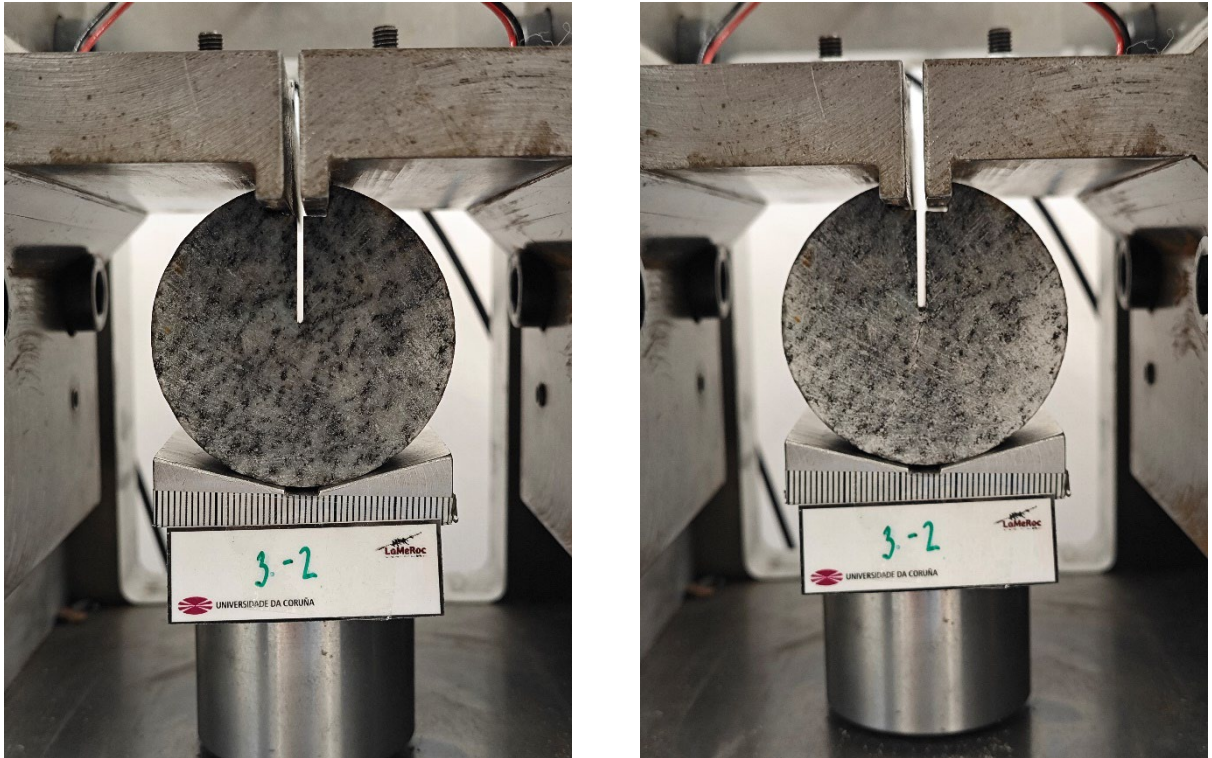
Figure A2-27. *Sample KFM01D (2-3) before (left) and after (right) the pCT test. The KIC value obtained was of 2.21 MPa m$^{1/2}$ obtained for a maximum load of 1329 N*
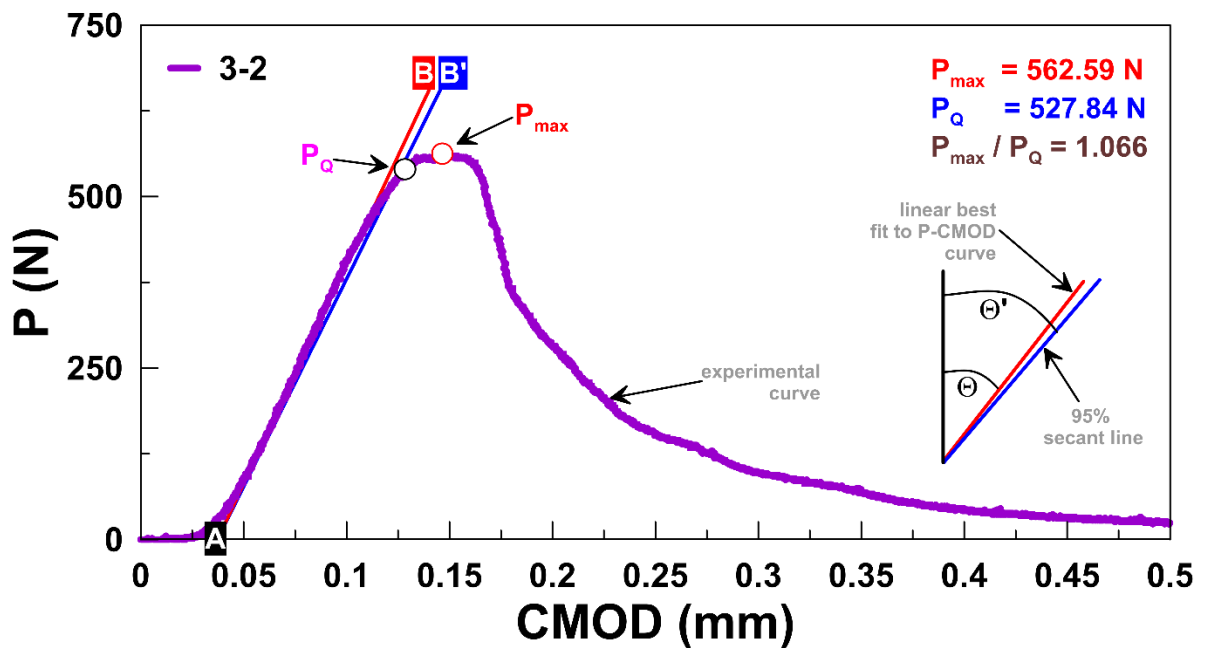

Figure A2-28. *Experimental results of the pCT test performed with specimen 2-3 and verification of the linearity criterion of the compliance method. See text for explanation.*

Notes: *P = applied horizontal load; **P$_{max}$** = maximum load; **P$_Q$** = conditional load; **CMOD** = crack mounth opening displacement (≡ load point displacement).*
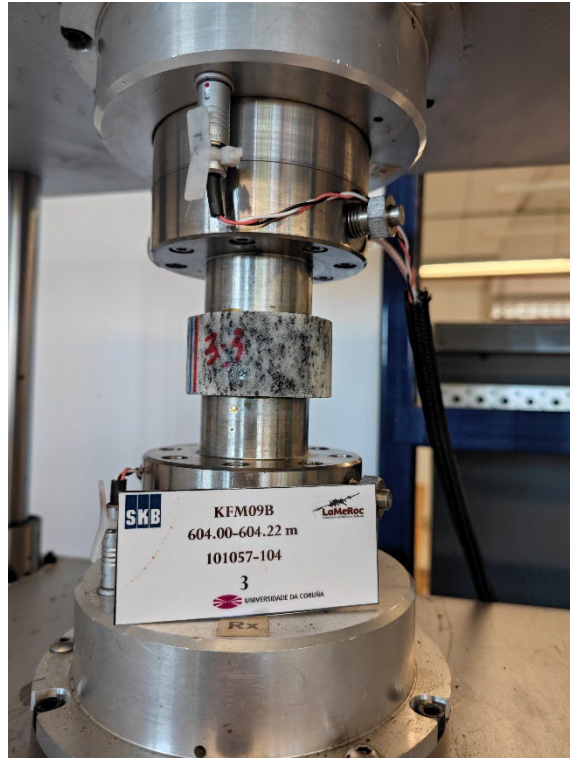
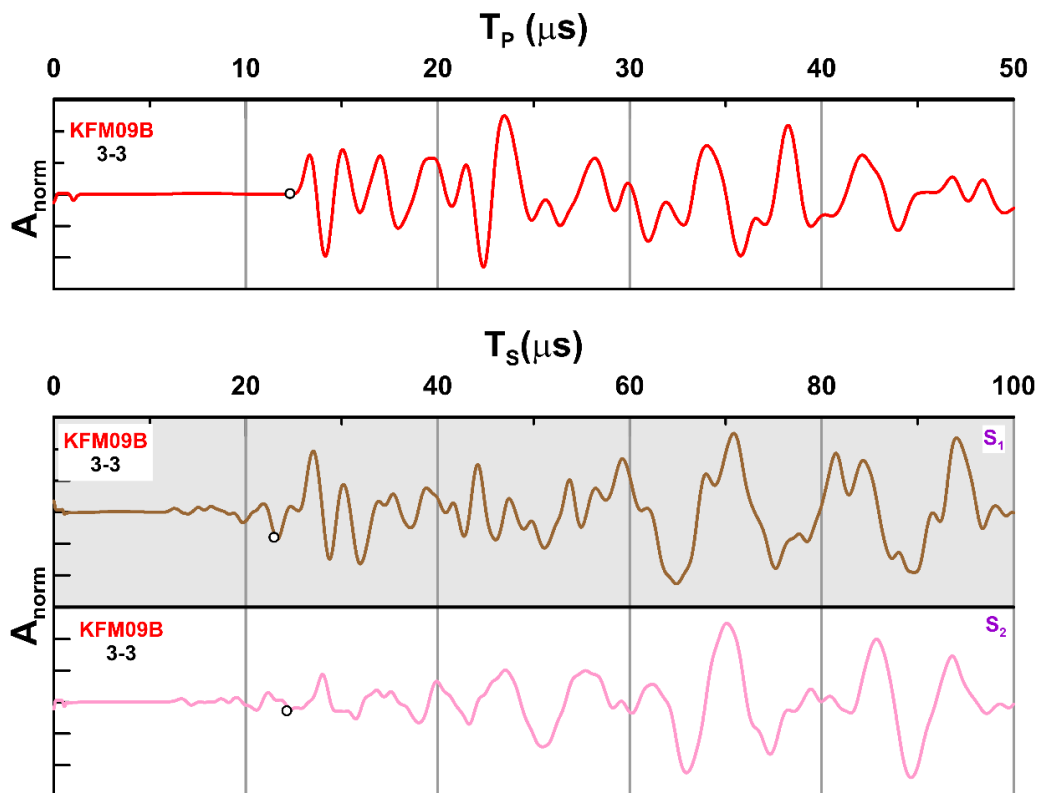**Figure A2-29.** *Measurement of ultrasonic velocities of sample KFM01D (2-4)*

Figure A2-30. *Experimental results of ultrasonic wave velocities (UWV) performed with specimen 2-4*

Figure A2-31. *Sample KFM01D (2-4) before (left) and after (right) the pCT test. The KIC value obtained was of 2.04 MPa m$^{1/2}$ obtained for a maximum load of 1293 N*

Figure A2-32. *Experimental results of the pCT test performed with specimen 2-4 and verification of the linearity criterion of the compliance method. See text for explanation.*

Notes: *P* = *applied horizontal load;* ***P$_{max}$*** = *maximum load;* ***P$_Q$*** = *conditional load;* ***CMOD*** = *crack mounth opening displacement (≡ load point displacement).*

Figure A2-33. Measurement of ultrasonic velocities of sample KFM09B (3-1)

Figure A2-34. Experimental results of ultrasonic wave velocities (UWV) performed with specimen 3-1
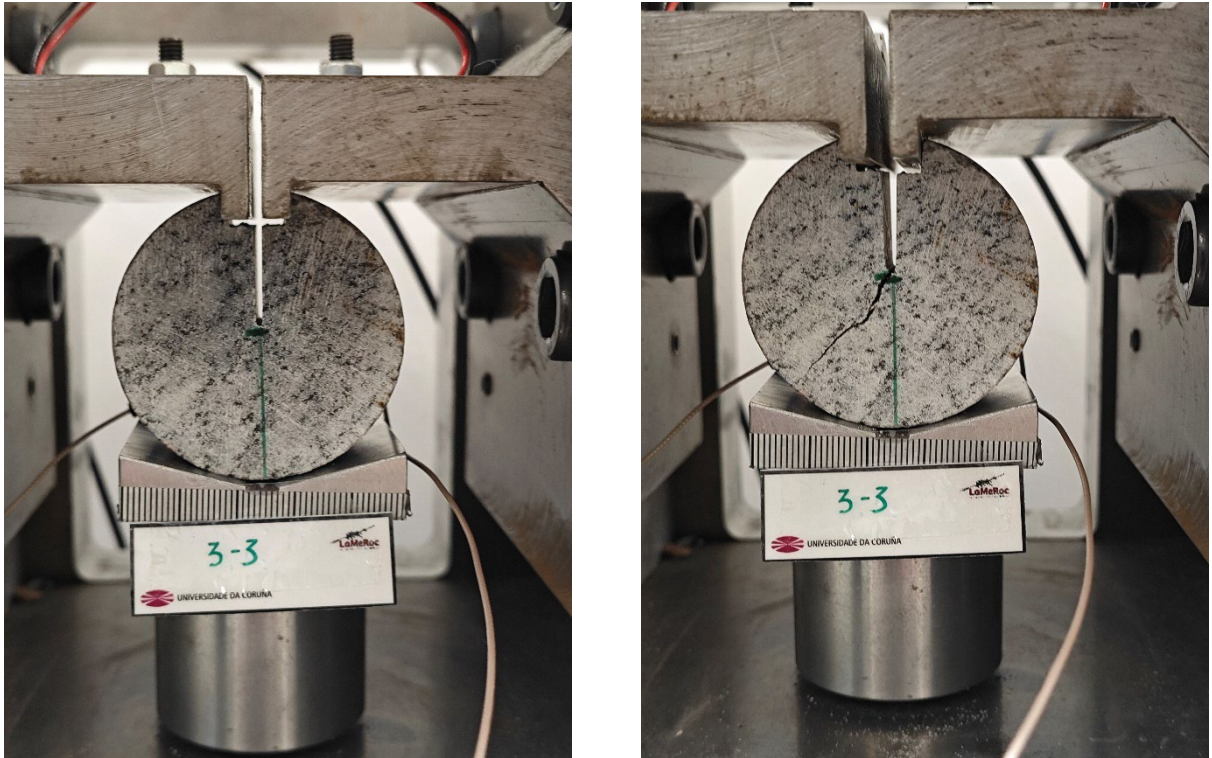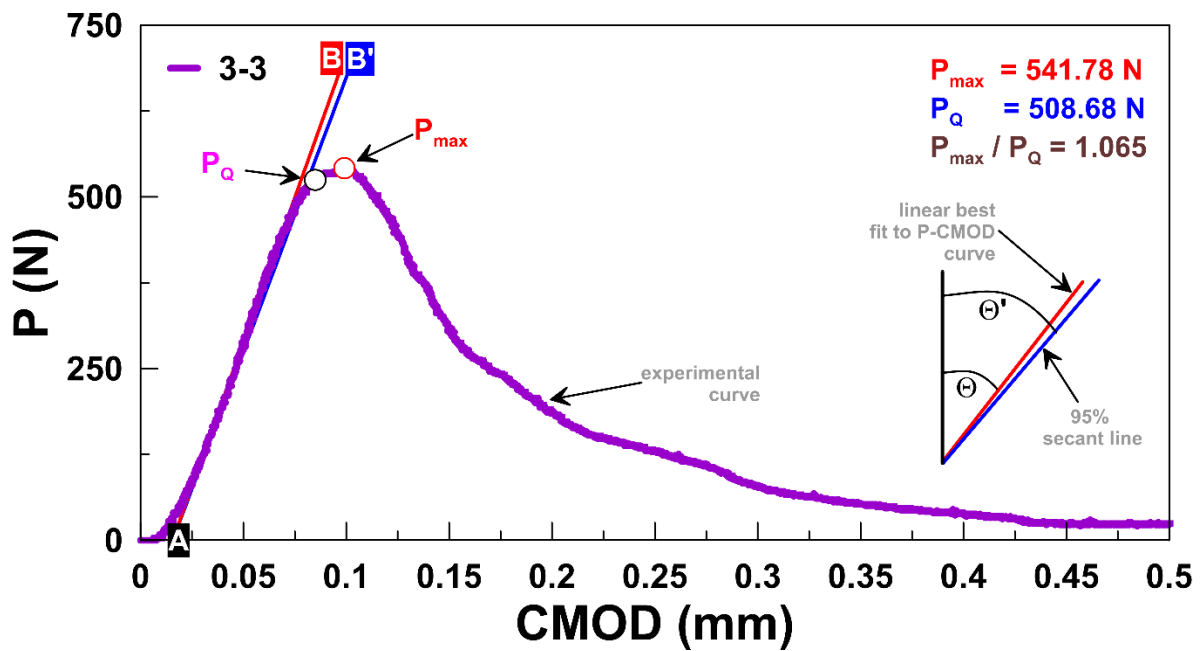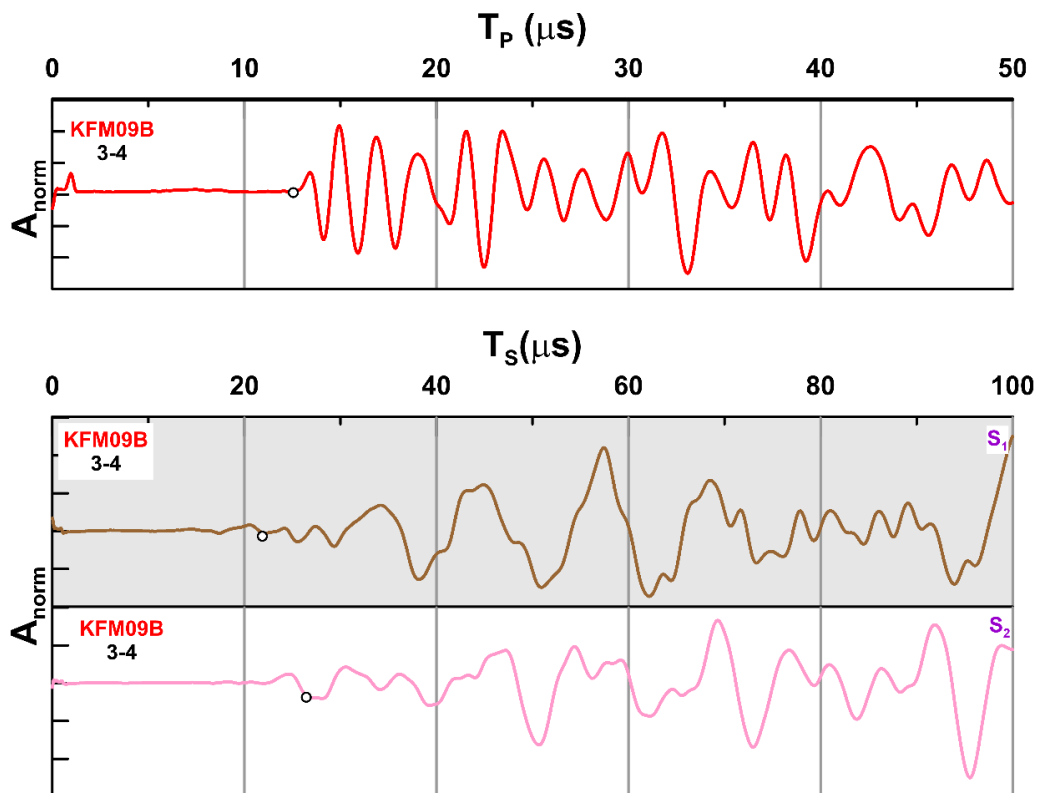
Figure A2-35. *Sample KFM09B (3-1) before (left) and after (right) the pCT test. The KIC value obtained was of 0.78 MPa m$^{1/2}$ obtained for a maximum load of 507 N*

Figure A2-36. *Experimental results of the pCT test performed with specimen 3-1 and verification of the linearity criterion of the compliance method. See text for explanation.*

Notes: P *= applied horizontal load;* **P$_{max}$** *= maximum load;* **P$_Q$** *= conditional load;* **CMOD** *= crack mounth opening displacement (≡ load point displacement).*

Figure A2-37. *Measurement of ultrasonic velocities of sample KFM09B (3-2)*

Figure A2-38. *Experimental results of ultrasonic wave velocities (UWV) performed with specimen 3-2*
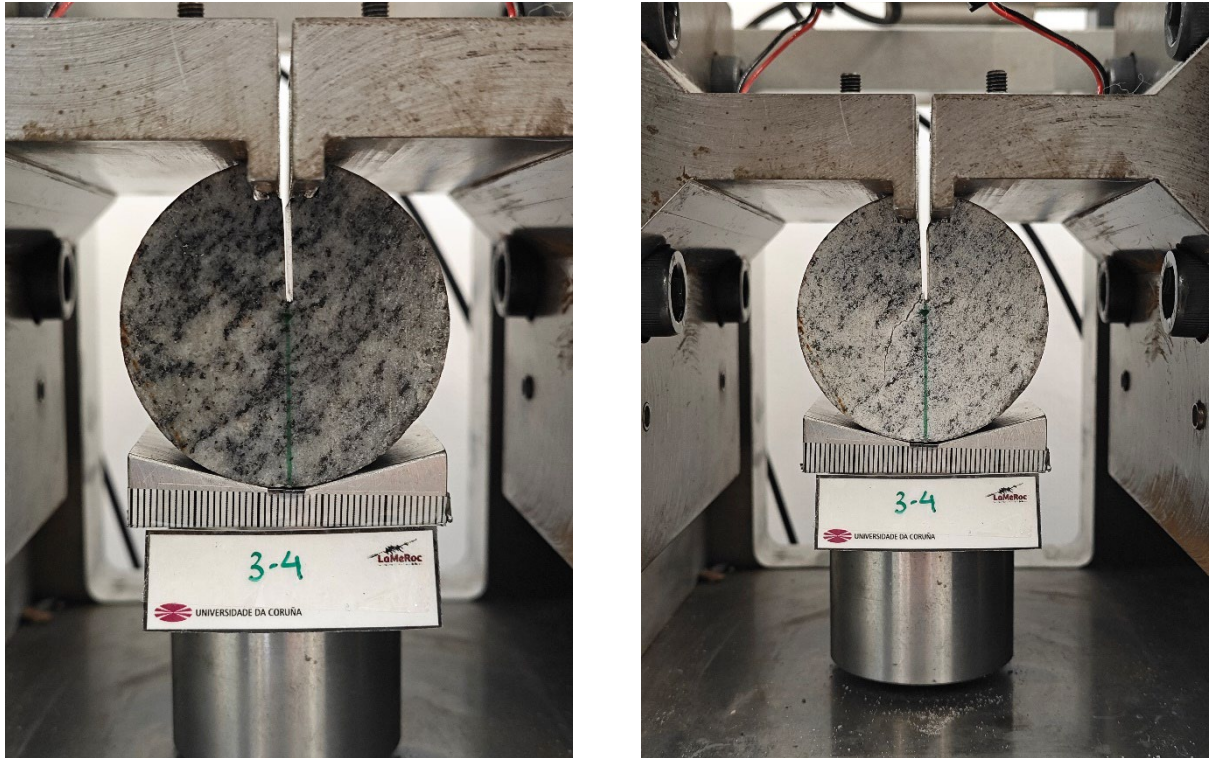
Figure A2-39. *Sample KFM09B (3-2) before (left) and after (right) the pCT test. The KIC value obtained was of 0.83 MPa m$^{1/2}$ obtained for a maximum load of 563 N*
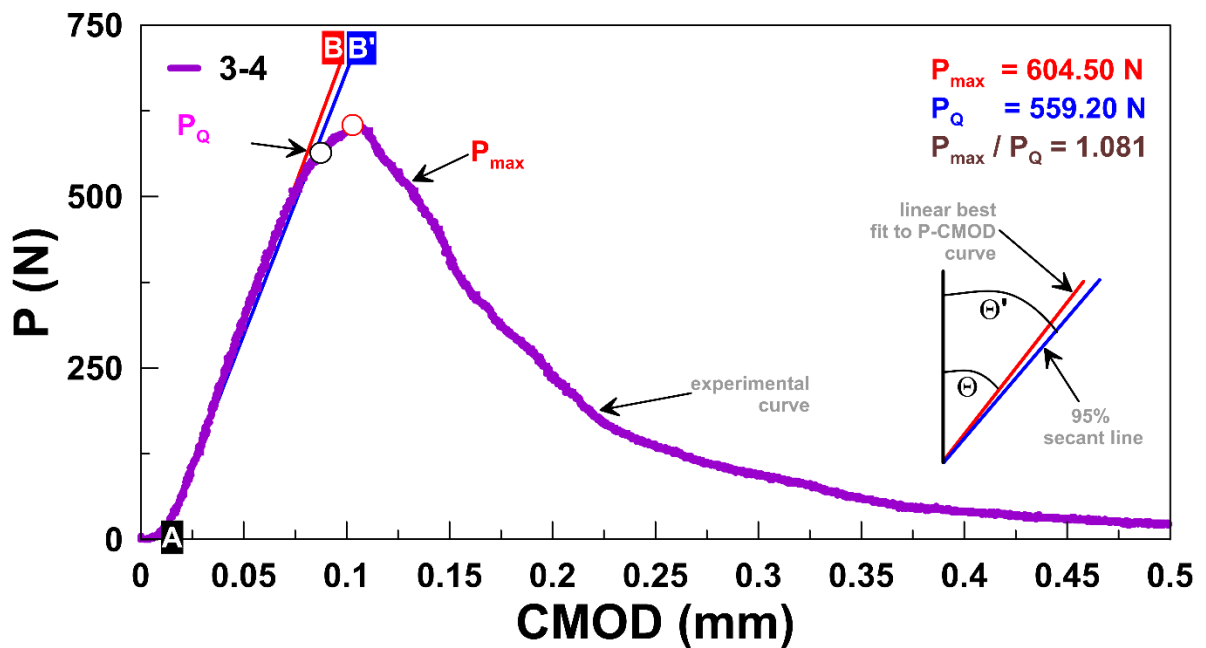

Figure A2-40. *Experimental results of the pCT test performed with specimen 3-2 and verification of the linearity criterion of the compliance method. See text for explanation.*

Notes: P = *applied horizontal load;* **P$_{max}$** = *maximum load;* **P$_Q$** = *conditional load;* **CMOD** = *crack mounth opening displacement (≡ load point displacement).*

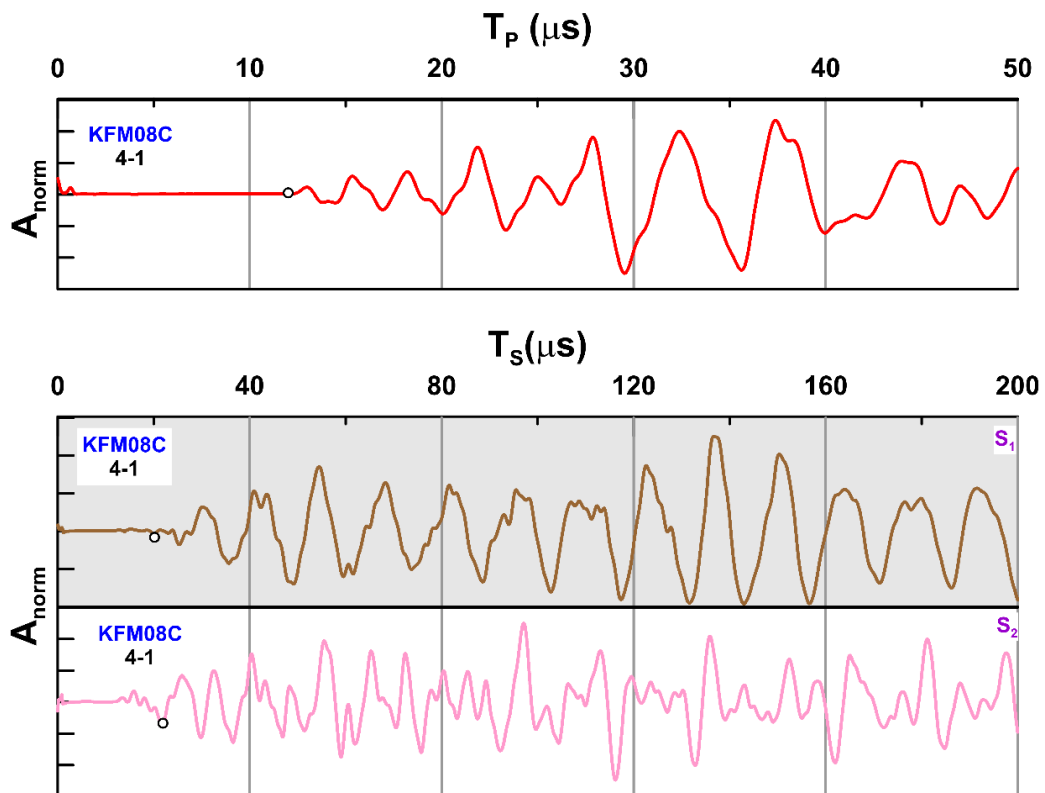**Figure A2-41.** *Measurement of ultrasonic velocities of sample KFM09B (3-3)*

Figure A2-42. *Experimental results of ultrasonic wave velocities (UWV) performed with specimen 3-3*
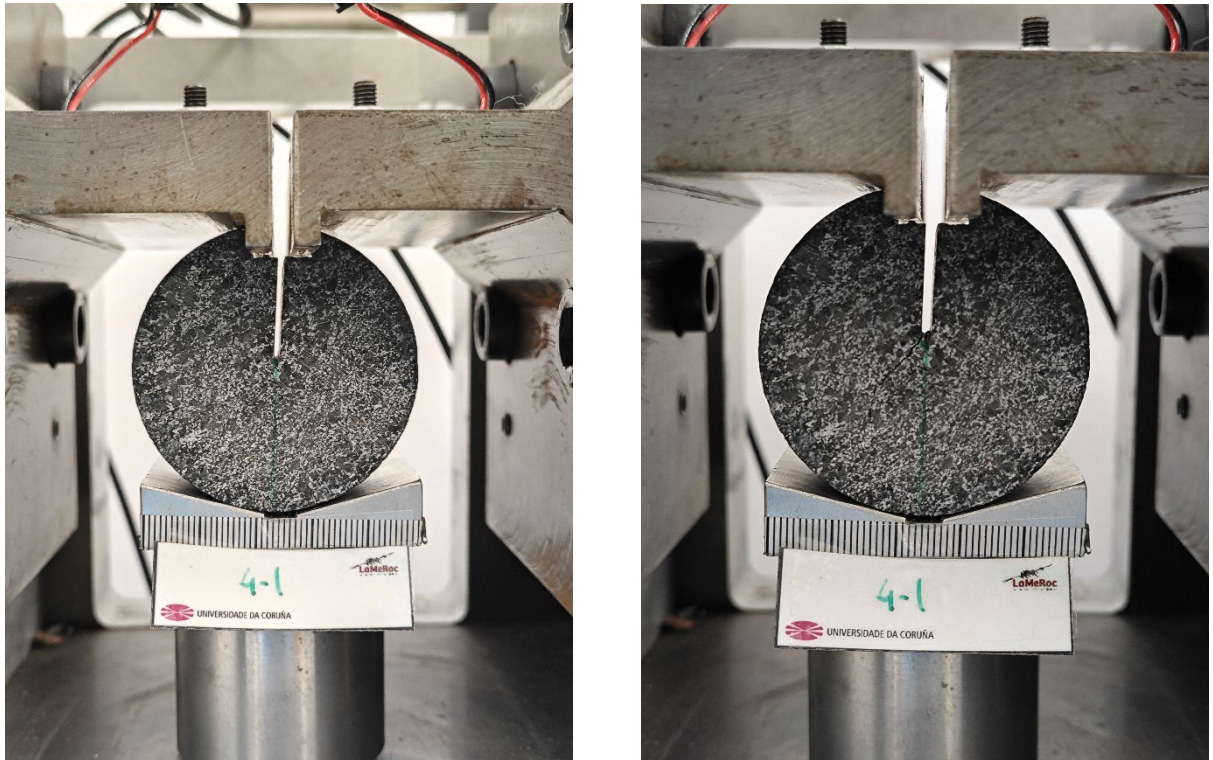
Figure A2-43. *Sample KFM09B (3-3) before (left) and after (right) the pCT test. The KIC value obtained was of 0.79 MPa m$^{1/2}$ obtained for a maximum load of 542 N*
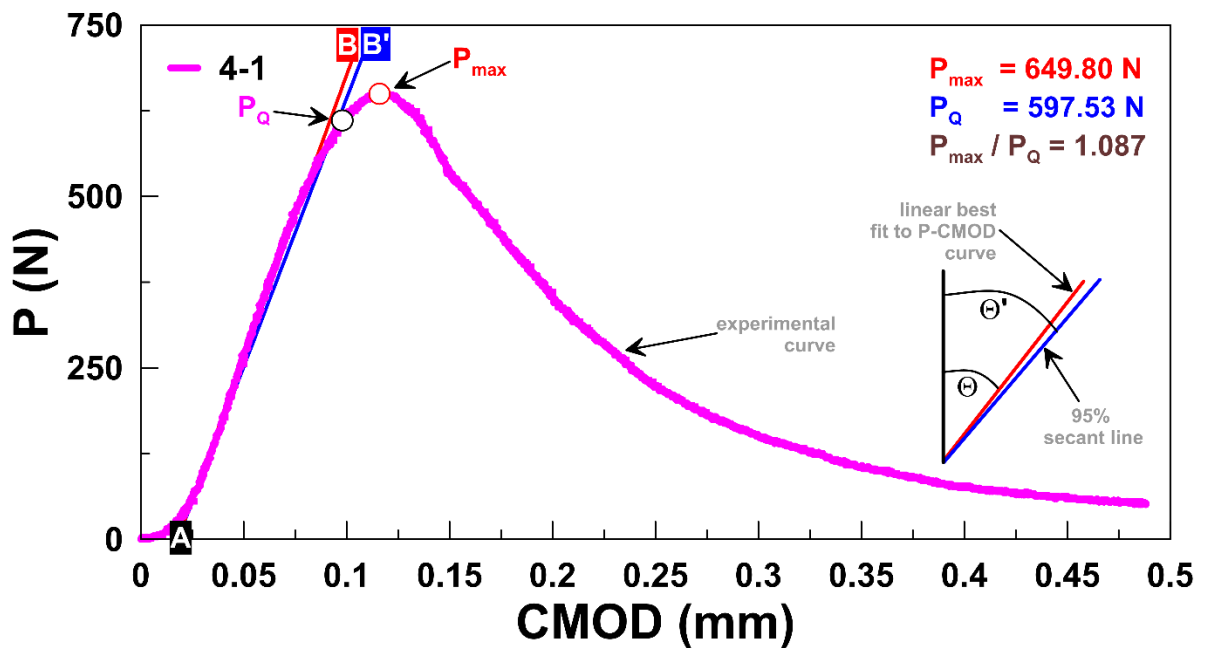

Figure A2-44. *Experimental results of the pCT test performed with specimen 3-3 and verification of the linearity criterion of the compliance method. See text for explanation.*

Notes: *P = applied horizontal load; **P$_{max}$** = maximum load; **P$_Q$** = conditional load; **CMOD** = crack mounth opening displacement (≡ load point displacement).*

Figure A2-45. *Measurement of ultrasonic velocities of sample KFM09B (3-4)*

Figure A2-46. *Experimental results of ultrasonic wave velocities (UWV) performed with specimen 3-4*

Figure A2-47. Sample KFM09B (3-4) before (left) and after (right) the pCT test. The KIC value obtained was of 0.87 MPa $m^{1/2}$ obtained for a maximum load of 605 N

Figure A2-48. Experimental results of the pCT test performed with specimen 3-4 and verification of the linearity criterion of the compliance method. See text for explanation.

Notes: P = applied horizontal load; **P_{max}** = maximum load; **P_Q** = conditional load; **CMOD** = crack mounth opening displacement ($\equiv$ load point displacement).

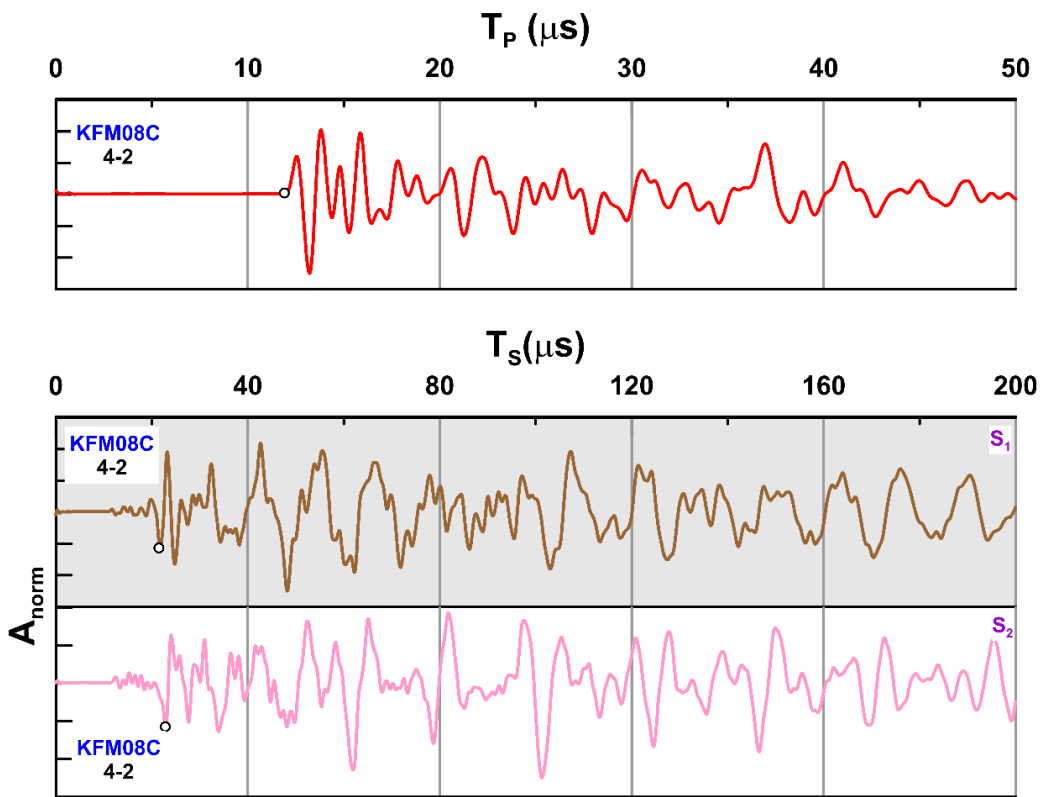**Figure A2-49.** *Measurement of ultrasonic velocities of sample KFM08C (4-1)*

Figure A2-50. *Experimental results of ultrasonic wave velocities (UWV) performed with specimen 4-1*
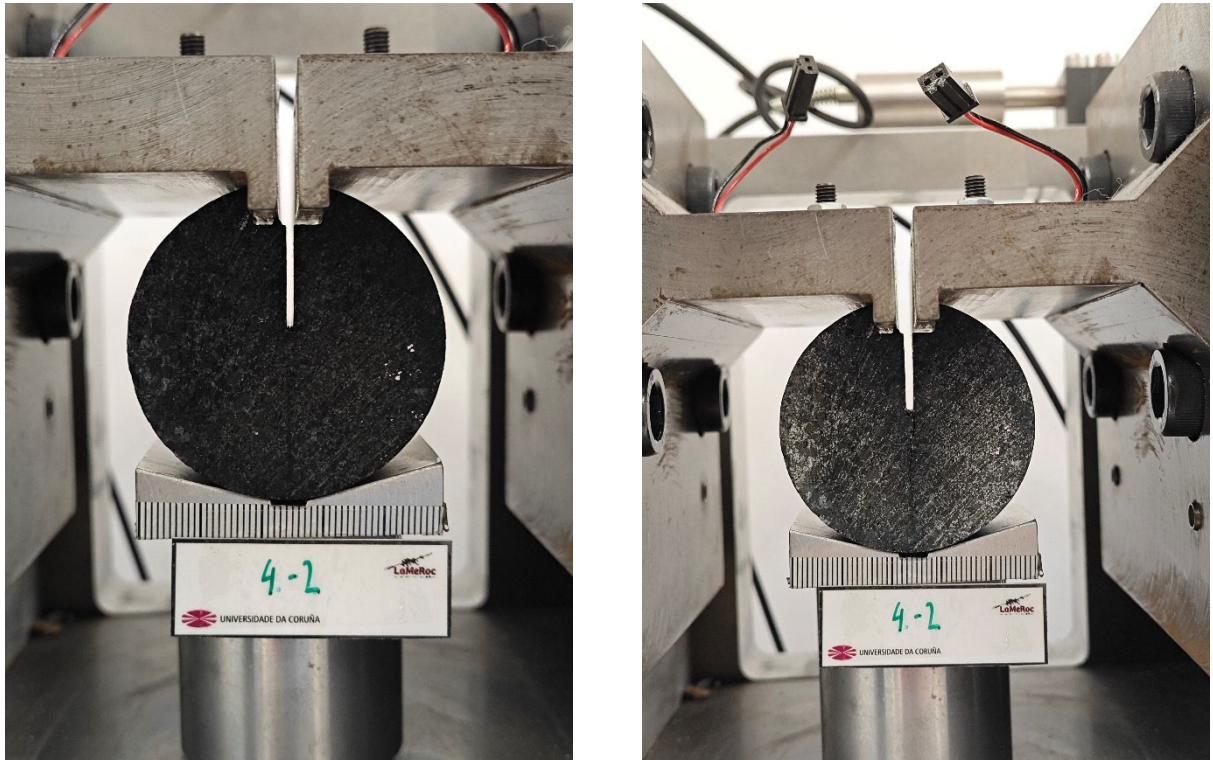
Figure A2-51. *Sample KFM08C (4-1) before (left) and after (right) the pCT test. The KIC value obtained was of 0.93 MPa $m^{1/2}$ obtained for a maximum load of 650 N*
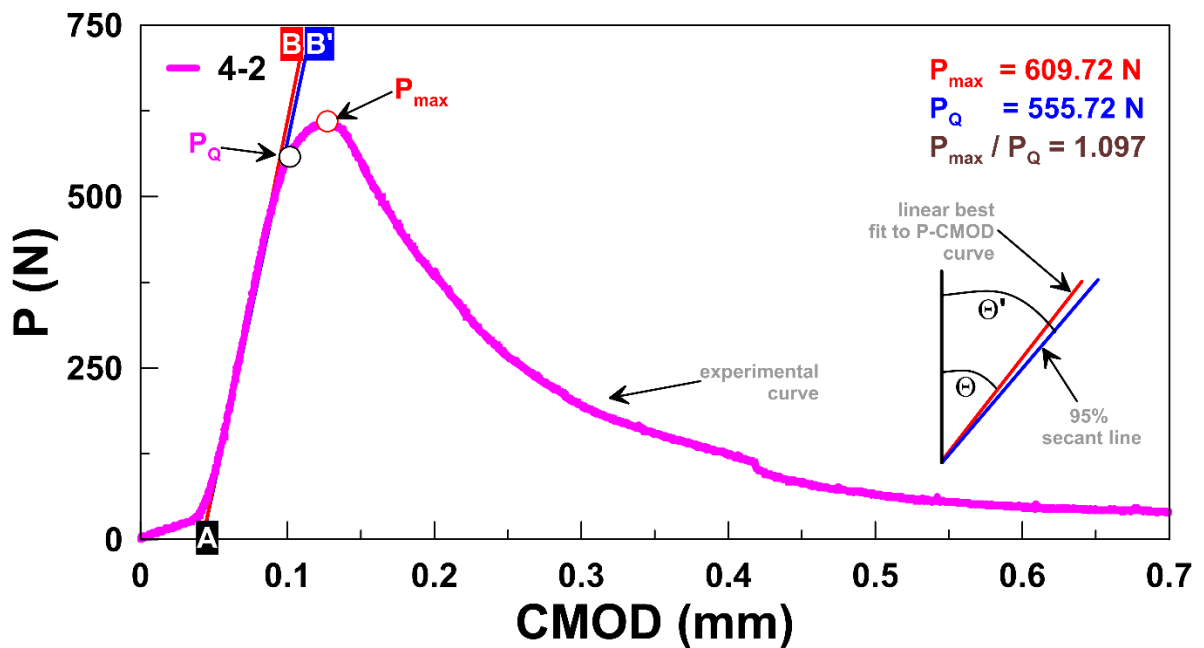

Figure A2-52. *Experimental results of the pCT test performed with specimen 4-1 and verification of the linearity criterion of the compliance method. See text for explanation.*

Notes: *P = applied horizontal load; P_{max} = maximum load; P_Q = conditional load; CMOD = crack mounth opening displacement ($\equiv$ load point displacement).*

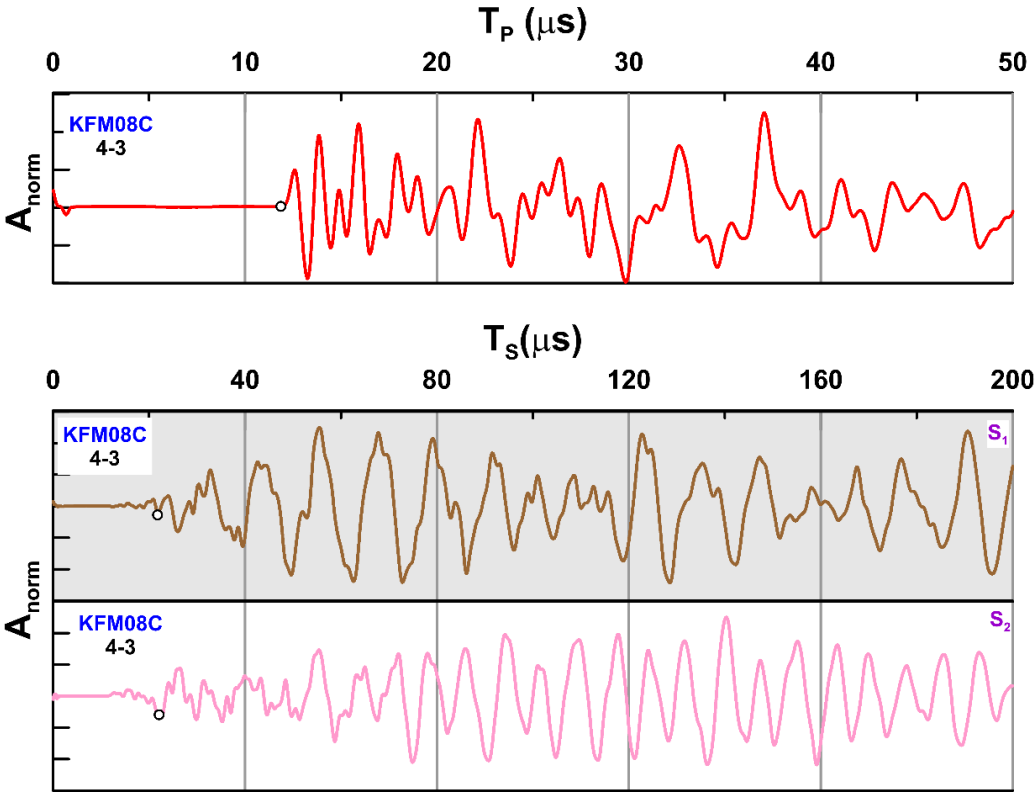*Figure A2-53. Measurement of ultrasonic velocities of sample KFM08C (4-2)*

Figure A2-54. Experimental results of ultrasonic wave velocities (UWV) performed with specimen 4-2
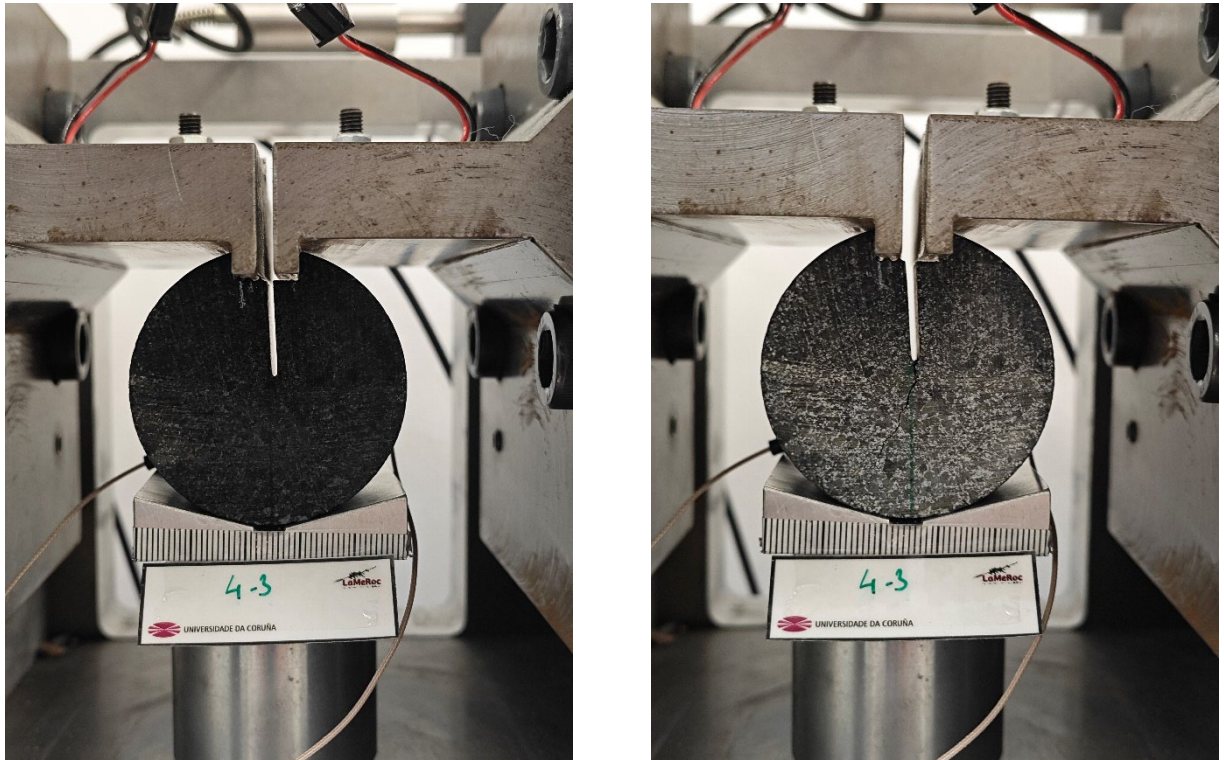
Figure A2-55. *Sample KFM08C (4-2) before (left) and after (right) the pCT test. The KIC value obtained was of 0.84 MPa m^{1/2} obtained for a maximum load of 610 N*
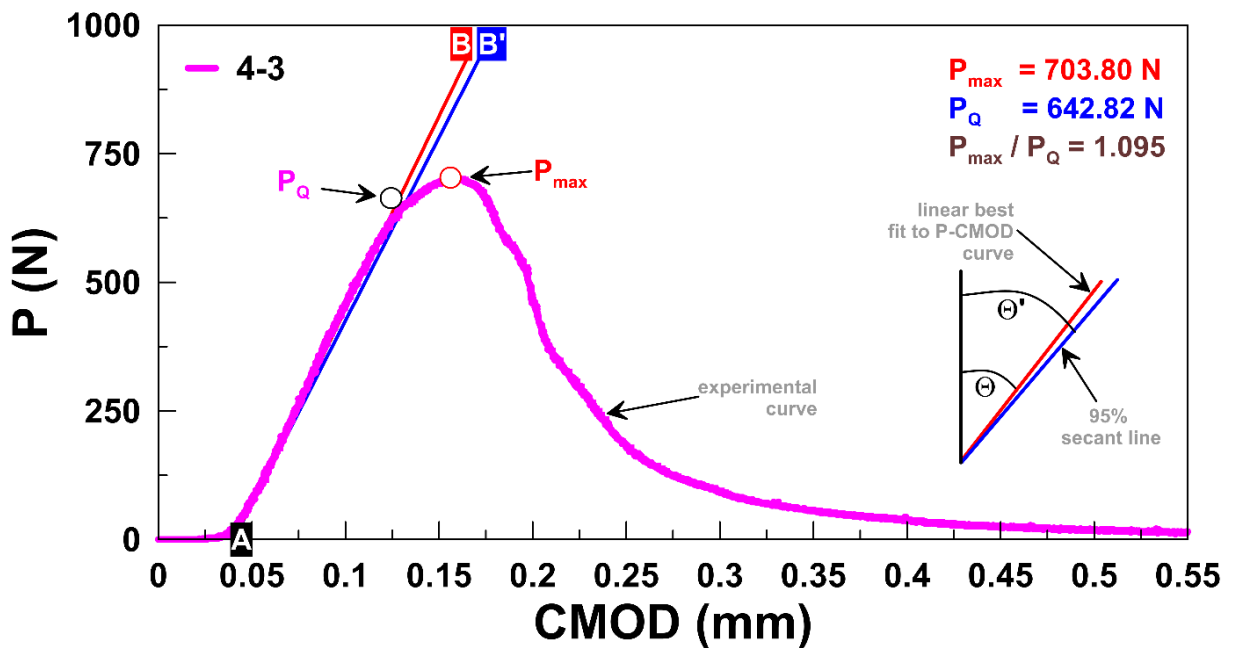

Figure A2-56. *Experimental results of the pCT test performed with specimen 4-2 and verification of the linearity criterion of the compliance method. See text for explanation.*

Notes: P = applied horizontal load; **P_{max}** = maximum load; **P_Q** = conditional load; **CMOD** = crack mounth opening displacement (≡ load point displacement).

Figure A2-57. *Measurement of ultrasonic velocities of sample KFM08C (4-3)*

Figure A2-58. *Experimental results of ultrasonic wave velocities (UWV) performed with specimen 4-3*

Figure A2-59. *Sample KFM08C (4-3) before (left) and after (right) the pCT test. The KIC value obtained was of 0.98 MPa m$^{1/2}$ obtained for a maximum load of 704 N*

Figure A2-60. *Experimental results of the pCT test performed with specimen 4-3 and verification of the linearity criterion of the compliance method. See text for explanation.*

Notes: P = *applied horizontal load;* **P$_{max}$** = *maximum load;* **P$_Q$** = *conditional load;* **CMOD** = *crack mounth opening displacement (≡ load point displacement).*

Figure A2-61. *Measurement of ultrasonic velocities of sample KFM08C (4-4)*
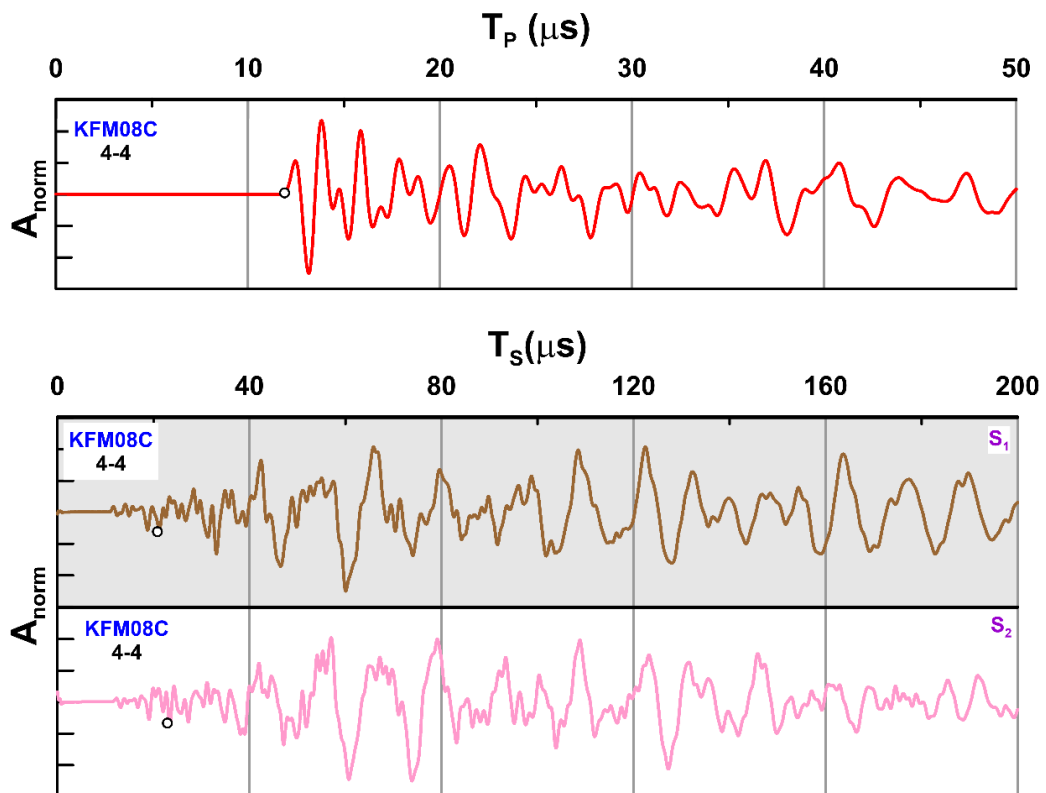

Figure A2-62. *Experimental results of ultrasonic wave velocities (UWV) performed with specimen 4-4*
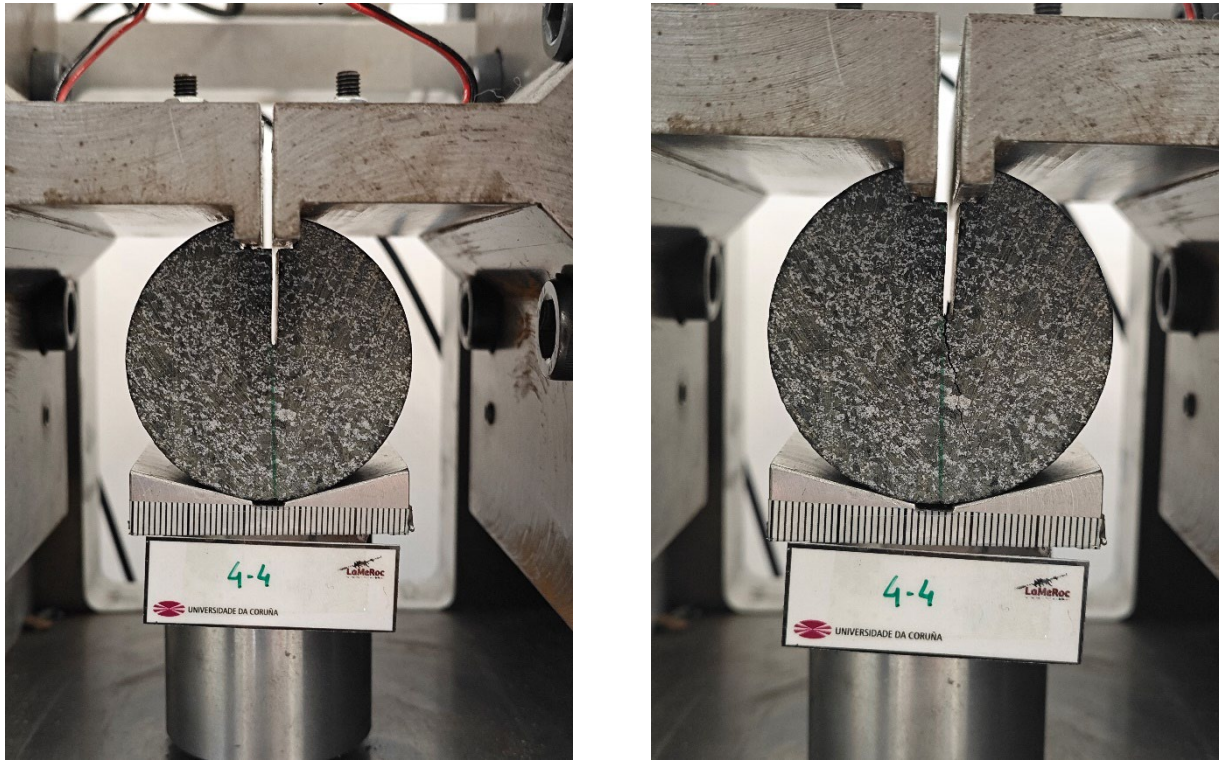
Figure A2-63. *Sample KFM08C (4-4) before (left) and after (right) the pCT test. The KIC value obtained was of 1.26 MPa m$^{1/2}$ obtained for a maximum load of 856 N*
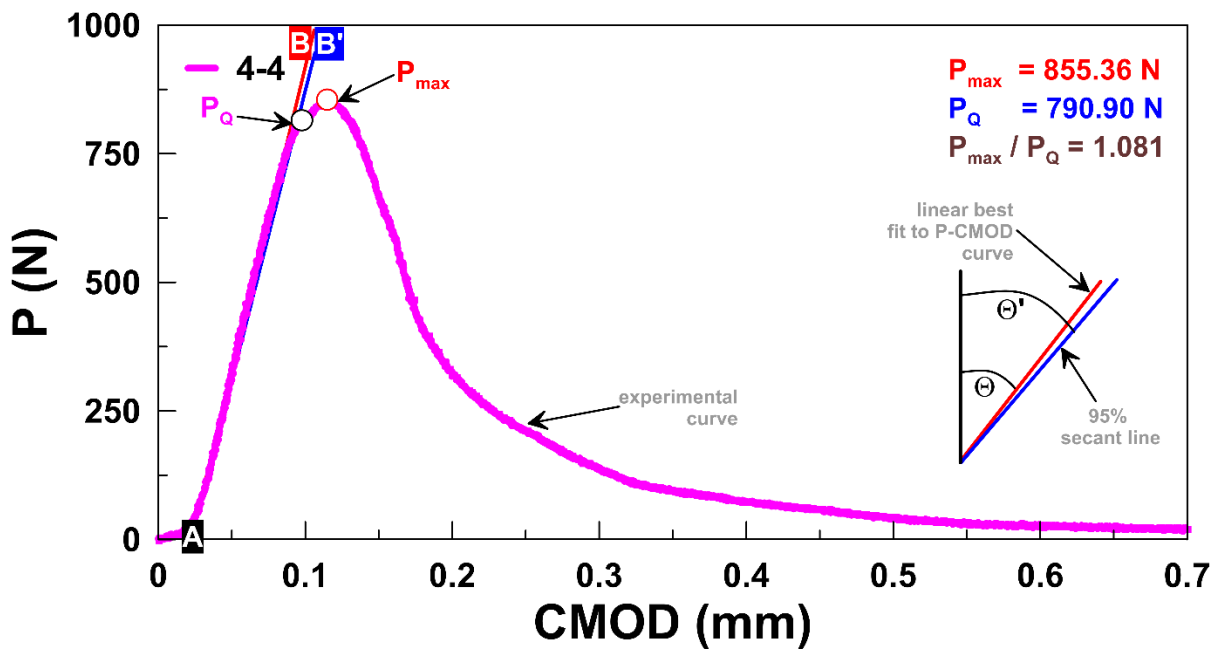

Figure A2-64. *Experimental results of the pCT test performed with specimen 4-4 and verification of the linearity criterion of the compliance method. See text for explanation.*

Notes: *P = applied horizontal load; P_{max} = maximum load; P_Q = conditional load; CMOD = crack mounth opening displacement (≡ load point displacement).*